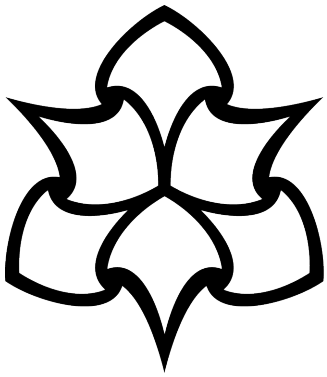

eScience 2 (2022) 365–381

Contents lists available at ScienceDirect

eScience

journal homepage: www.keaipublishing.com/en/journals/escience

Review

Additive manufacturing (3D printing) of electrically conductive polymers and polymer nanocomposites and their applications

Kirstie R. Ryan, Michael P. Down, Nicholas J. Hurst, Edmund M. Keefe, Craig E. Banks *

Faculty of Science and Engineering, Manchester Metropolitan University, Chester Street, Manchester, M1 5GD, UK

HIGHLIGHTS

- Additive manufacturing offers a unique solution for fabricated complex geometries.
- Conductive polymers can be processed with additive manufacturing for conductive applications.
- This review summarizes the relevant achievements in the additive manufacturing of conductive polymers.
- The prospective applications of these additive manufacturing printed conductive materials are explored.

GRAPHICAL ABSTRACT

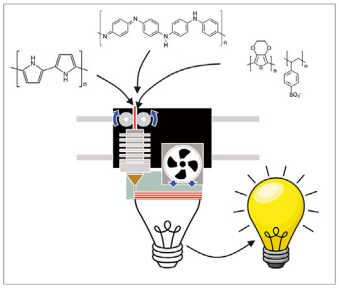

ARTICLE INFO

Keywords:
Conducting polymers
Additive manufacturing
Electrochemcial applications
Supercapacitors
Batteries

ABSTRACT

Additive manufacturing, or three-dimensional (3D) printing, offers a unique solution for fabricating complex geometries with high tolerances. Currently, many commercial additive manufacturing machines focus on the printing of polymers with limited functionalities. However, conductive polymers (CPs) can be processed to enable the additive manufacturing of conductive, low-density, and low-cost parts for a myriad of applications. This review summarizes the relevant achievements in the additive manufacturing of conductive polymers (CPs) and conductive polymer nanocomposites, with a discussion of the advantages and limitations of processing and printing these materials compared with alternative traditional manufacturing methods and their properties. Finally, the prospective applications of these additive manufacturing printed conductive materials are explored.

1. Introduction

Additive manufacturing (AM) has revolutionized the way we manufacture components and products across a myriad of industries, including electronics, aerospace, biomedical, wearable technologies, fashion, and automotive. From the conceptualization of a three-dimensional (3D) model to the manufacture of a printed part, AM allows industries to efficiently and quickly realize their designs for commercial applications at relatively low costs. Unlike traditional manufacturing methods, AM does not require the use of tooling and dies to produce parts, which also potentially reduces material waste and labor costs. One area that has gained attention is the AM of electrically conductive materials that can be used in electronics, biomedical devices, and wearable technologies, to name just a few. Although carbon-based and metallic nanomaterials are often combined with polymers in AM [1–3], electronically conductive polymeric materials can offer a novel solution, as they are known to be lightweight, versatile and low cost.

Conductive polymers (conjugated polymers) consist of chains of repeating units of monomers, where the atomic structure has been changed to enable them to conduct electricity; for example, polypyrrole (PPy), poly(3,4-ethylenedioxythiophene): polystyrene sulfonate

* Corresponding author.
E-mail address: c.banks@mmu.ac.uk (C.E. Banks).

https://doi.org/10.1016/j.esci.2022.07.003
Received 26 December 2021; Received in revised form 13 June 2022; Accepted 22 July 2022
Available online 4 August 2022

Abbreviations

AM	additive manufacturing
CNF	carbon nanofiber
CNT	carbon nanotube
CP	conductive polymer
CSA	camphorsulphonic acid
DBSA	dodecylbenzenesulfonic acid
DIW	direct ink writing
DLP	direct light projection
EHD-Jet	electrohydrodynamic jetting
FDM	filament deposition modelling
FFF	fused filament fabrication
GO	graphene oxide
HDPE	high-density polyethylene
HIP	high-impact polystyrene
MAG	micro-architected graphene
MEA	microelectrode arrays
MWCNT	multi-walled carbon nanotube
PANI	polyaniline
PBT	polybutylene terephthalate
PCB	printed circuit board
PDMS	polydimethylsiloxane
PE	polyethylene
PEDOT:PSS	poly(3,4-ethylenedioxythiophene): polystyrene sulfonate
PEGDA	poly(ethylene glycol) diacrylate
PLA	polylactic acid
PLLA	poly-L-lactic acid
PMMA	polymethyl methacrylate
PP	polypropylene
PPy	polypyrrole
PμSL	projection micro-stereolithography
RFID	radio frequency identification
SLA	stereolithography
SLS	select laser sintering
UDMA	urethane dimethylacrylate
UTS	ultimate tensile strength

(PEDOT:PSS), polyaniline (PANI), and polyacetylene are widely reported electrically conductive polymers. Although these polymers are intrinsically conductive, they often require the use of doping to attain high electrical conductivities that can rival those of metals. To further enhance the electrical conductivity of a polymer, secondary conductive filler materials such as carbon [4,5], graphene [1], and silver [6,7] are often incorporated. This approach can be used to create conductive polymer composites using specialized polymers with tailored chemical and physical properties.

In this paper, we provide a review of intrinsically conductive polymers and polymer-based composites used in AM, with a focus on the processing, electrical performance, and applications of these conductive materials. The review starts from the overview of various AM techniques by clarifying their strengths and weaknesses. Then three intrinsically conductive polymers (CPs), including PANI, PPy, and PEDOT:PSS, are discussed from the aspects of basic properties, synthesis methods, and applicability for AM techniques, and strategies of enhancing conductivity, followed by AM of these conductive polymers. We next summarize the AM of conductive polymer nanocomposites, in which various metallic nanoparticles and carbon-based nanomaterials have been used as additives to enhance the conductivity of products by AM. Finally, the applications of CPs and polymer nanocomposites by AM, in areas of bioelectronics, flexible and stretchable electronics, sensors, and electrochemical devices, are highlighted with representative progress. We prospect that future AM of CPs and nanocomposites will focus on the improvement on both electrical conductivity and mechanical properties with more upgraded technologies.

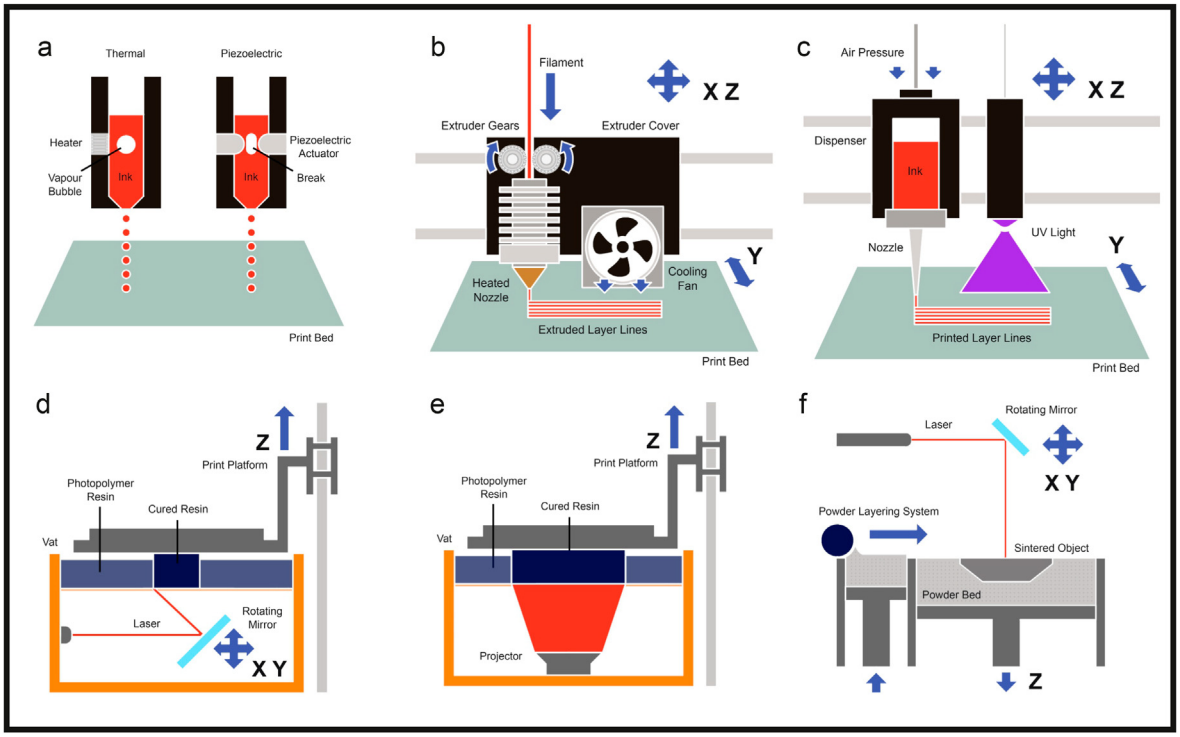

Fig. 1. Schematic overview of various additive manufacturing techniques: (a) inkjet [18], (b) FFF/FDM [19], (c) DIW [20], (d) SLA [21], (e) DLP, (f) SLS [22].

2. Additive manufacturing

The basic principle of additive manufacturing builds by adding materials in a layer-by-layer fashion, where the layers are two-dimensional (2D) slices taken from a 3D Computer Aided Design (CAD) model. There are six main methods of AM, each offering different finishes, resolutions, and physical properties. From the reported literatures, the main methods of AM include extrusion-based systems — such as filament deposition modelling (FDM), sometimes referred to as fused filament fabrication (FFF), as well as direct ink writing (DIW) and inkjet printing — and polymerization systems, such as stereolithography (SLA) and direct light projection (DLP), and finally powder-bed fusion selective laser sintering (SLS); Fig. 1 presents a schematic overview of these methods [8–13]. The vat polymerization technique offers smooth-surface finishes as well as robust, watertight prints due to strong bonding between layers and fine resolutions. The main limitation with vat polymerization is the use of only a single resin formulation, which must be photocurable. These resins often consist of a monomer with a functional end group such as an acrylate, which will be polymerized in combination with a photo initiator (P.I.) that creates radicals upon exposure to UV radiation. The efficiency of photocuring is dependent on the P.I, concentration, power from the UV laser, and molecular weight. It should be noted that when filler materials are dispersed within the resin, the consequent scattering effects will lead to under-curing. This phenomenon can be tailored by adjusting the P.I. concentration, matching the refractive index of the filler to the polymer, and controlling the size and shape of the filler [14–17].

Direct-ink writing uses a liquid-phase ink that can be cured chemically with UV radiation or thermal treatment. The key requirement for DIW printing is that the ink should maintain a shear-thinning behavior while flowing out from the nozzle, followed by quick elastic recovery upon reaching the build plate to build self-supporting structures. This means that many DIW inks need to be carefully adjusted to the right viscoelastic properties, which often appear as pastes or gels with high viscosities in the range of 10^3–10^5 Pa s at low shear rates [23,24]. When printing with filler materials, the size, concentration, and dispersions are critical for the viscosity and flow dynamics of the ink. Depending on the geometry, even small quantities can lead to a rapid increase in viscosity.

Fused filament fabrication (FFF) is an extrusion-based technology like DIW, using a spool of filament that is extruded through a heated nozzle onto a build platform. Speed of printing and cooling, as well as thermal transitional temperatures such as melting temperature are the key printing considerations when using FFF. It is one of the most commonly used printing technologies and is seen across a myriad of applications due to its low cost [25]. Inkjet printing uses a nozzle to print out droplets of ink onto a substrate via thermal or piezoelectric methods. Important factors that affect the outcome of the print include contact angle, density, ink viscosity, and speed of printing. Inkjet printing of filler materials can lead to print heads becoming blocked by a build-up of filler material at the opening of the nozzle. Therefore, similarly to DIW, the size, geometry, and concentration need to be carefully considered for good printability.

Selective laser sintering (SLS) is a process involving a laser to selectively sinter or melt powders, which fuses the particles of the powder together in a thin layer [26]. A build platform then drops down, and a roller is used to deposit a new layer of particles on top to continue the printing process, creating a 3D object in a layer-by-layer fashion [27]. The surrounding unfused powders act as the supports to the solid object, so there is no need to design supports into the build file. SLS can be used on both metals and thermoplastics, however, SLS printed parts are usually subjected to rough surface finishes and high degrees of warpage and shrinkage [28]. All the above methods require some degree of post-processing, which can include the removal of support material, post-curing processes in UV or thermal ovens, and/or general cleaning and polishing of the part for aesthetic purposes.

3. Intrinsically conductive polymers

Intrinsically conductive polymers (CPs), a group of organic materials, can be a novel alternative to the traditional conductive materials, such as metallic and carbonaceous materials. CPs can demonstrate low densities and excellent processibilities and can act as cost-effective and efficient conductive base materials [29–32]. They have a broad range of applications, including biomaterials for tissue engineering and biomedical devices [33], sensors [34], transistors, electromagnetic interference shielding [35], light-emitting diodes, photovoltaic cells [36], supercapacitors [37], batteries [38], and artificial muscles [39]. CPs are electrically conductive because they have conjugated structures of repeatedly alternating monomer units of double and single bonds along the molecular structure [40], see Fig. 2. In CPs, three out of four valance electrons form strong σ bonds through hybridization of the sp^2 orbital, resulting in strongly localized electrons. The remaining electrons sit in the p_z orbital, which overlaps with neighboring p_z orbitals, forming π bonds. The conjugated system of a continuous set of p_z orbitals results in the delocalization of π electrons, similar to the delocalization of electrons in metals, which allows the electrons to move freely, resulting in electrical conductivity [30]. Although these conjugated polymers are intrinsically conductive, their conductivity can be increased by orders of magnitude with the use of p and n dopants [33,41].

There are many variations of conjugated polymers, but the three main CPs used in AM are PANI, PPy, and PEDOT:PSS, each of which we will briefly describe.

3.1. PANI

PANI has many advantages over other intrinsically conducting polymers, such as its low cost to manufacture, ease of synthesis, good environmental stability, and tunable properties; see Table 1 [42,43]. These qualities have attracted the exploration of PANI in AM techniques as either a primary material or a filler material for AM conducting polymers [44,45]. PANI can be synthesized and modified in a number of ways, permitting applications in various areas, such as sensors [46], electronics [47], electrochemical [48], thermoelectric [49], biomedical [50], corrosion [51], and light emitting diodes [52], making PANI an exciting CP for AM electrically conductive materials for commercial applications [53]. PANI is synthesized via two main approaches: chemical and electrochemical. In chemical oxidation polymerization, PANI is synthesized

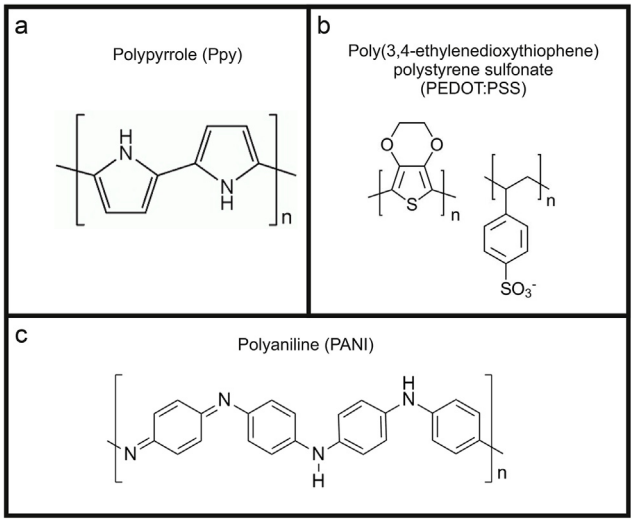

Fig. 2. Chemical structure of conductive polymers PPy (a), PEDOT:PSS (b), and PANI (c).

Table 1
Properties of commonly used conjugated polymers in additive manufacturing.

Polymer	Conductivity (S cm^{-1})	Doping type	Properties	Ref.
PPy	10^{2}–10^{3}	p	nontoxic and biocompatible, high electrical conductivity	[185], [59], [186]
PANI	10^{-1}–10^{3}	p, n	inexpensive, easy to synthesize, good conductivity, environmentally stable	[185], [187], [188]
PEDOT:PSS	10^{-1}–10^{3}	p, n	transparent, excellent thermal and chemical stability, high conductivity	[185], [189], [79], [80], [190]

by using hydrochloric acid (HCl) or sulfuric acid (H_2SO_4) as a dopant and ammonium persulfate (APS) as an oxidant in an aqueous environment [53,54]. Electrochemical preparation usually applies potentiodynamic and galvanostatic techniques to electrodeposit PANI onto an electrode surface.

Like many other π-conjunctive polymers, PANI can be difficult to process due to its insolubility and infusibility, caused by stiffness in the main polymer chain. This can limit the commercial applications of PANI, as the mechanical and electrical properties of the polymer are compromised [54]. There are methods of tackling this issue, making PANI easier to process for AM, such as making modifications to PANI to include functional polar groups in the polymer backbone, which results in an increase in solubility and infusibility [55]. Polymer hybrids/composites of PANI and thermoplastics have also been used to help improve its processibilities [56]. This technique often uses in situ polymerization of PANI or the grafting of polymers onto PANI. In some cases, fibers or particles of PANI are incorporated into a polymer matrix to achieve a consistent network for conductive polymer composites [57]. Through the development of polymer/PANI composites, improvements can be realized in the mechanical, electrical, and thermal properties compared to PANI alone [58–60]. Finally, the most widely used method of improving the solubility of PANI is through doping [61,62]. For example, adding protonic organic acids such as dodecylbenzenesulfonic acid (DBSA) [55,63] or camphorsulphonic acid (CSA) [64,65] greatly improves the solubility of PANI in non-polar solvents.

3.2. PPy

PPy is one of the most extensively studied CPs due to its high electrical conductivity (see Table 1), ease of synthesis, and good environmental stability [66–69]. Polypyrrole is also a non-toxic and biocompatible material, garnering much interest in the biomedical field [70]. Polypyrrole is a π-conjunctive polymer and therefore has problems with solubility and infusibility, hindering the processing of PPy for AM techniques. Similar to PANI, PPy can also be modified to improve the processing and solubility of PPy and its derivatives. This is achieved by modifications to the monomer, co-polymerization, and doping [71]. These methods affect the overall electrical, mechanical, and physiochemical properties of the polymer. Large dopants can be added to reduce intermolecular interactions of PPy chains and improve solubility, however, this often leads to a decrease in electrical conductivity, as charge carriers have further to travel between chains [72]. Nevertheless, dopants such as dodecylbenzene sulfonic acid (DBSA), di(2-ethylhexyl) sulfosuccinic acid sodium salt (NaDEHS), and poly(2-acrylamido-2-methyl-1-propane sulfonic acid) (PAMPS) are commonly used to improve and enhance the properties of polypyrrole [73–75].

The polymerization of pyrrole into polypyrrole can be achieved through chemical oxidation, electrochemical oxidation, and photopolymerization, for instance. In chemical oxidation, pyrrole is polymerized using $FeCl_3$ or other iron (III) or copper (II) salts [72,76]. In contrast, in electrochemical polymerization, the monomer is dissolved within a solvent with an anionic doping salt. When an anodic potential is applied, the monomer oxidizes at the surface of a suitable electrode surface [76–78]. PPy is unique in that in situ polymerization can occur with exposure to UV light, making PPy an interesting material for light-based AM techniques such as SLA, DLP, SLS, and UV-assisted DIW [79,80]. To improve upon its intrinsic properties for commercial applications, PPy can be combined with another polymer to form a composite that is mechanically robust and can be processed, easily widening the scope of potential applications. Reported PPy–polymer composites have included PPy/PEGDA for printed electronics [81], as well as PPy/PP and PPy/PE composites for improving the electrical properties and flexibility of inherently brittle PPy [82,83]. For example, Ma et al. reported on a PPy/PLLA composite that they additively manufactured for tissue engineering applications [66]. The ability to polymerize PPy using a variety of dopants and methods, along with the vast amount of potential PPy composites available, creates an extensive list of applications both on a research level and commercially, including supercapacitors [84], electronic devices [85], protection against corrosion [86], biomedical devices [87], solar cells [88], fuel cells [89], and electromagnetic interference (EMI) shielding [90].

3.3. PEDOT:PSS

PEDOT:PSS, a type of polythiophene (π-conjunctive polymer), is a very promising CP with excellent thermal and chemical stability, low production cost, corrosion resistance, thermal stability, biocompatibility, flexibility, good transparency, and high conductivity; see Table 1 [91,92]. PEDOT can be synthesized by chemical oxidation and electrochemical polymerization from the monomer EDOT [93]. PEDOT alone is not soluble and therefore can be difficult for solution processes. However, this issue can be overcome by adding PSS to PEDOT, resulting in a water-soluble electrically conductive polymer [94]. In this polymer blend, PSS acts as a dopant and stabilizer by forming soluble polyelectrolyte complexes with PEDOT [94]. Similar to PANI and PPy, PEDOT:PSS can be blended with other polymers to form hybrids and composites to further improve their mechanical and processing properties. For instance, the reported conductivity of PEDOT:PSS can be enhanced with the addition of polyols such as glycerol and sorbitol, resulting in conductivities that are orders of magnitude higher [94]. PEDOT:PSS triblock copolymer blends (Pluronic 123) have also been reported in the fabrication of stretchable electrodes with improved electrical conductivities of ~1700 S/cm [95]. Applications of PEDOT:PSS found in industry include electronic textiles [96], photocatalysis [97], transparent electrodes [95], solar cells [98], supercapacitors [92], anti-static coatings [99], photovoltaics [100], and fuel cells [101].

Overall, each of the intrinsically conductive polymers discussed above offers good conductivities that can be used in a myriad of applications, from fuel cells to electronic textiles. For AM purposes, the main concern about CPs is their ability to be processed sufficiently for different printing technologies. However, as discussed, the use of carefully considered dopants and polymer blends significantly improves this ability, resulting in AM-functional CPs.

4. Additive manufacturing of conductive polymers

Additive manufacturing of CPs offers an interesting combination of functional materials and precision manufacturing that can be applied in advanced applications. However, as previously mentioned, π-conjunctive polymers are difficult to process, which can create issues with the AM of CPs. Each AM method has a unique set of requirements to achieve good printability, including specific transitional temperatures as well as rheological and chemical properties [102]. Therefore, CPs are often blended with other polymers to enable AM whilst still maintaining electrical functionality [9]. This, however, usually means a reduction in

the material's overall electrical conductivity due to the presence of a secondary insulating polymer [103]. To improve upon the polymer's overall conductivity, conductive particles such as carbon, graphene, silver, etc. are added [104].

4.1. Additive manufacturing of PANI

The printing of CPs has become an interesting field in academia and industry, as complex functional parts can be manufactured quickly with minimal waste for a whole host of applications. Some of the reported major achievements in this field have included work by Joo et al., who recently demonstrated the AM of PANI/polyurethane composites via DLP (Fig. 3a) [105]. This study found that the addition of 6 wt% PANI nanofibers to the PU matrix decreased the sheet resistance from 1.08×10^{-11} to 9.28×10^{-7} Ω/sq. The mechanical properties of the composites were also improved, with a reported Young's modulus of 26.1 MPa (6 wt % PANI) compared to 24.3 MPa for pristine PU. The elongation at break of the composite was also increased from 5.20×10^{2} (pristine PU) to 5.76×10^{2} (6 wt% PANI), providing an improvement not only in toughness but also in flexibility.

4.2. Additive manufacturing of Ppy

Yamada et al. reported the AM of PPy into a Nafion® sheet using a Ti/sapphire laser (λ = 850 nm) (Fig. 3b) [106].They used multi-photon excitation of tris(2,2'-bipyridyl)ruthenium complex $[Ru(bpy)_3^{2+}]$ by a femtosecond pulse laser with near infrared wavelength as the light source, the multi-photon sensitized polymerization of pyrrole, and an AM (photo-fabrication) system of polypyrrole (PPy) by 3D scanning of the laser focal point. In this study, the AM of PPy into a Nafion® sheet was carried out to evaluate the electronic conductivity of the product micro-structures formed by multi-photon sensitized polymerization. This method of micro-nano AM created high resolutions with a minimum line width of approximately 0.8 μm. The multi-photon sensitized polymerization of PPy resins also achieved extremely high conductivities of up to 4.1×10^{3} S m^{-1}, tested using the 2-point probe method under a vacuum. Yamada et al. [106] studied the relationship between laser power, line width, and conductivity (Fig. 3b(i,ii)) and found that the line width and conductivity of the AM composite increased along with the increasing laser power. This was believed to be due to polymer chain orientation and crystallinity, stimulated by an increase in the electric field from the femto-laser. Each AM technique can offer a different resolution and finish to the printed part and therefore a difference in mechanical, electrical, and thermal properties [107,108], in contrast to the extremely fine resolutions achieved by Yamada et al. [106].

4.3. Additive manufacturing of PEDOT:PSS

Gutiérrez-Fernández et al. achieved a line width of ≈25 μm for their AM PEDOT:PSS onto indium tin oxide (ITO) substrates using inkjet printing [109]. In this study, thin films of poly(3, 4-ethylenedioxythiophene) complexed with poly(styrenesulfonate) (PEDOT:PSS) on indium tin oxide (ITO) were prepared by inkjet printing technology. The process allowed the creation of thin films over large areas. A relatively broad range of thicknesses could be obtained by the addition of subsequent polymer layers in what resembled an additive manufacturing process. The resulting inkjet PEDOT:PSS films were homogeneous in regard to both electrical and mechanical properties. In inkjet printing, the line width is closely related to the diameter of the ejected droplets. Following on from this work, they reported that their printed thin films were homogeneous and had reasonable electrical and mechanical stability (Fig. 3c). The Young's moduli of the films were measured to be between 4.6 ± 0.2 GPa for one printed layer and 2.4 ± 0.1 GPa for four printed layers, and their recorded moduli values were higher than with other manufacturing approaches, such as free-standing

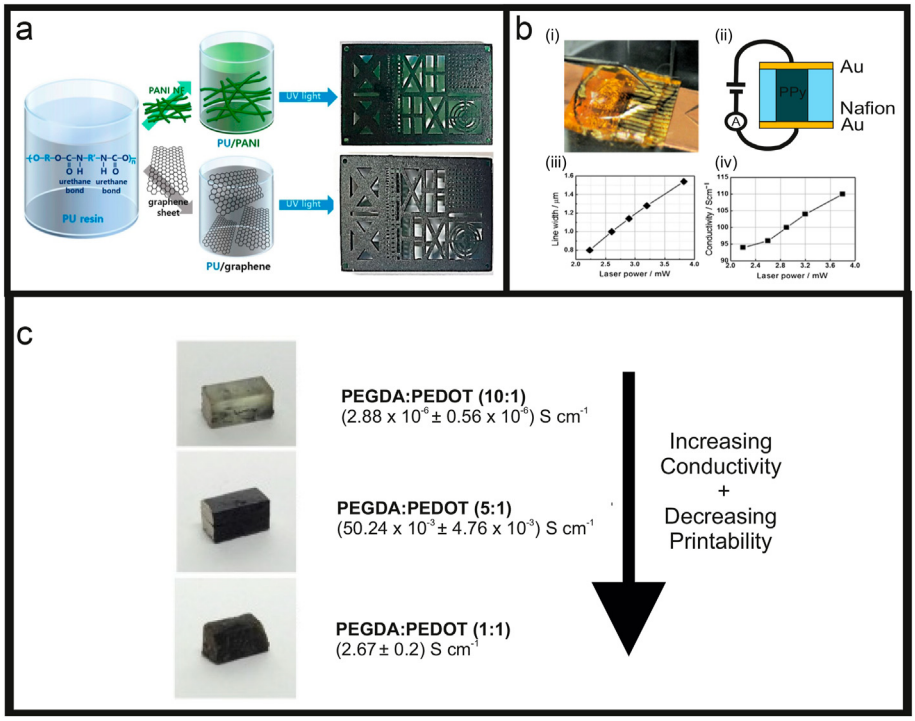

Fig. 3. (a) Schematic of the overall process of conductive AM polyurethane (PU)/polyaniline (PANI) nanofiber (NF) and a graphene sheet (GS), including photographs of the composites (Copyright© The Royal Society of Chemistry [100]). (b) (i) Photograph of the Nafion® sheet after immobilization of Au electrodes, and (ii) schematic of the conductivity measurement. Relationships between the incident laser power, the line width of the PPy straight lines (iii), and the conductivity of the PPy straight lines (iv) (Copyright© ACM, 2019 [106]). (c) Conductivity at different PEDOT ratios in a resin matrix (PEGDA + 1 wt% PI + DMSO 5%). Inset: images of the printed blocks at different PEDOT ratios in the PEGDA matrix, including electrical conductivity (Copyright© Elsevier, 2019 [111]).

fabrication [110].

Scordo et al. reported the effects on electrical performance when varying the concentration ratio of PEGDA to conductive PEDOT (10:1, 5:1, 1:1), see Fig. 3 [111]. Their findings showed that an increase in the concentration of PEDOT (1:5) improved electrical conductivity (Fig. 3), but the mechanical performance of the composite inks was compromised, hindering the overall printability. The 5:1 ink showed the most promise. This is often seen in the development of conductive polymers and composites for AM — there is a compromise between printability and performance, and optimization is crucial [112–114].

Although there are many advantages of using AM techniques over traditional methods (casting and forming), such as high-precision complex parts, low costs, and minimal waste, there are still concerns about whether a layer-by-layer manufacturing approach can produce robust load-bearing parts compared to traditional manufacturing methods. Mohan et al. tested this concept by conducting a study on AM hybrid polyethylene-graphene nanoplatelets (6 wt%)-polypyrrole (2 wt%) composites compared to those that had been compression molded [11, 114]. The mechanical, thermal, and electrical performance of both manufacturing techniques was assessed, indicating that the mechanical properties of the AM composites exhibited a 13% reduction in tensile strength and a 31.8% reduction in flexural strength compared to the compression-molded samples. However, the AM samples did show an increase in electrical conductivity of 7.9% ($\sim 3 \times 10^{-4}$ S m^{-1}) compared to those that had been compression molded ($\sim 2.78 \times 10^{-4}$ S m^{-1}), owing to the potential alignment of filler material during the extrusion process in the AM (FFF) process.

An alternative technique to combine AM and CPs is via infiltration of a CP into a porous AM part during the post-processing stage. The AM component can be used to manufacture complex and intricate shapes, whilst infiltration of a CP in a secondary processing stage means that enhanced mechanical and electrical properties can be achieved without the need for extensive processing of the CP. Mu et al. utilized this technique in the AM of a commercial UV curable Spot E resin via DLP with sacrificial sodium chloride particulates mixed in Ref. [115]. Salt leaching was then used to create complex porous parts, which could be applied as a template for the infiltration PEDOT:PSS and 5 vol% ethylene glycol (EG) (Fig. 4). The resultant product was a flexible conductive component with tunable properties. The reported resistance of the composite was 50 kΩ, which meant that the AM part could light an LED bulb (Fig. 4b) [115].

The AM of CPs is summarized in Table 2, showing that a variety of technologies can be used to AM CPs and their composites. As previously discussed, the overall properties of the printed material can be greatly affected by the resolution, feature size, and conductive material component. As there is a broad scope of printing techniques and materials, this creates an abundance of possible applications for AM conductive materials.

5. Additive manufacturing of conductive polymer nanocomposites

Conductive fillers dispersed within a polymer matrix can be used as an alternative to conjugated polymers to provide electrical pathways to an intrinsically insulated polymer or aid in increasing the conductivity in CPs. The incorporation of these fillers can drastically affect all properties of the composite, including optical, mechanical, thermal stability, and electrical properties. The benefit of using conductive fillers in a polymer means that a wide range of polymers can be used as the matrix material; therefore, depending on the application, a bio-polymer can be used, or a polymer with specific mechanical, chemical, or optical properties. The polymers can also be tailored for specific AM techniques, including photocurable polymers for SLA, low-viscosity polymer resins for inkjet printing, and high-viscosity resins for DIW. This provides a degree of freedom for AM conductive polymer composites using a variety of technologies. The limitations of this method depend on the achievable

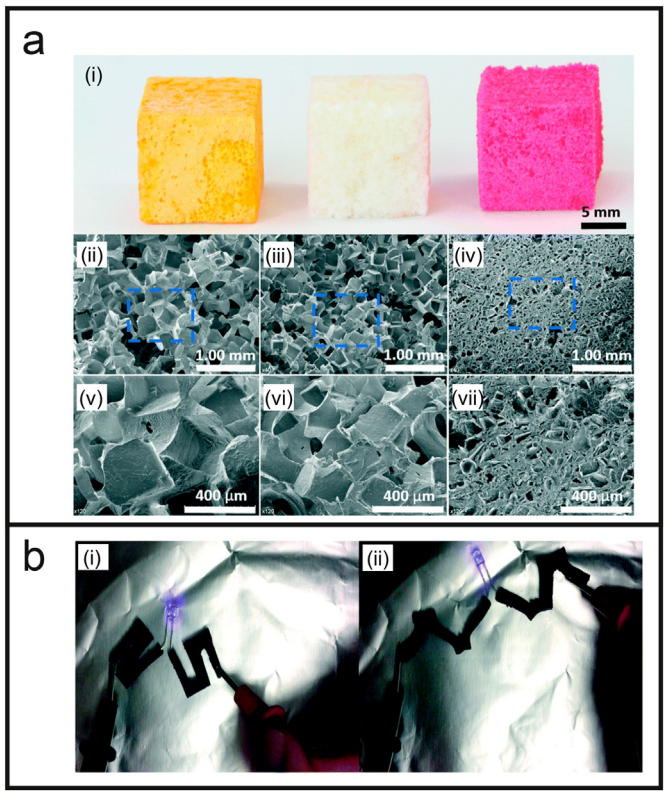

Fig. 4. (a) (i) From left to right, AM cubes using extra-fine PEGDA, and commercial resins Standard Clear and Spot-E. SEM images of the porous structures printed by using (ii) coarse, (iii) fine, and (vi) extra-fine Spot-E ink. (v), (vi), and (vii) are zoomed-in images of (ii), (iii), and (iv), respectively. (b) An LED bulb is lit up when voltage is applied through porous polymer materials infiltrated with PEDOT:PSS conductive ink, and (ii) the bulb keeps shining while the porous conductive material is stretched (Copyright© The Royal Society of Chemistry, 2017: [115]).

loading of fillers above the percolation threshold for electrical conductivity, and good dispersions of conductive fillers within the polymer matrix. These factors can affect the overall printability, attainable electrical conductivity, as well as mechanical, thermal, and chemical properties [116]. Another consideration is the cost of using expensive filler materials such as silver, gold, etc. [117,118].

The percolation threshold of the conductive filler in the polymer matrix is critical when developing conductive inks for AM. The percolation threshold is the transition between polymers changing from an electrically insulating state to an electrically conductive state. In polymer composites, conductive fillers are usually distributed randomly throughout the polymer matrix, which means that the composite can be either electrically insulating or conductive, depending on whether the concentration of fillers is below or above the percolation threshold [119]. Above the percolation threshold, a critical amount of conductive filler material enables the formation of one or more continuous conductive networks within the polymer, changing the electrical properties [120]. This critical amount is dependent on the type of filler material, geometrical factors (flakes, spheres, tubular particles), filler alignment, composite processing, and the polarity of the polymer matrix [118, 121–123]. We have summarized the AM of conductive polymer nanocomposites in Table 3.

5.1. *Metallic nanoparticles*

Metallic nanoparticles are the most obvious choice to utilize due to their known excellent conductivities, although they obviously are more expensive than carbon-based materials. In particular, the dispersion of

Table 2
Electrical properties of additive manufactured conductive polymers and their associated composites.

Conductive Polymer	Secondary Materials	Additive Manufacturing Technology	Electrical Properties (S cm^{-1})	Applications	Ref.
PEDOT:PSS	PEGDA matrix	SLA	0.05	microsensors, MEMS, and microfluidics devices	[111]
2-hydroxyethyl acrylate (HEA) with 4-vinylbenzenesulfonic acid (SSS), 3, 4-ethylenedioxythiophene (EDOT) (PHEA-PSS/PEDOT)	–	DLP	1.20	flexible sensors	[191]
PANI nanofibers (5 wt%)	polyacrylate and graphene (1.2 wt%)	DLP	4.00×10^{-9}	electronic and biomedical devices	[192]
PPy tubular nanoparticles (30%)	poly-l-lactide (PLLA)	DIW	7.50×10^{-5}	tissue engineering scaffolds	[66]
PEDOT	PEGDA (PEGDA:PEDOT 5:1)	customized SL printer	0.05	biosensors, energy storage, health monitoring, and sensing applications	[111]
PANI (1:3)	dodecylbenzenesulfonic acid (DBSA)	FFF	3.26	sensors and actuators	[10]
PPy	collagen and polyarylate film	inkjet	1.10	conducting polymer structures that promote cellular adhesion	[161]
PANI doped with MWCNTs	PU 5 wt%		45.0	organic antennae	[156]
Ppy doped with $Fe(ClO_4)_3$	Nafion sheet	multi-photon sensitized polymerization Ti/sapphire laser ($\lambda = 850$ nm) 3D printer laser	410	conductive inks for printed metamaterials	[106]
PEDOT(12 wt%):Nafion	Nafion and ABS blend	FFF	1.00×10^{-5}	organic electrochemical transistors (OECTs), wearable electronics, and electronic textiles	[168]
PEDOT:PSS	ionic liquid hydrogel	microreactive inkjet printing (MRIJP)	900	next-generation bioelectronic devices; wearable and stretchable electronic devices	[13]
EDOT (17 wt%)	PEGDA	two-photon lithography	0.04	photonic metamaterials, microfluidic and biomedical devices, MEMS, and actuators	[103]
PEDOT:PSS 1.25% (w/w)	multiwalled carbon nanotubes (MWCNTs) (0.5%), deionized water, glycerol, and ethylene glycol in a ratio of 8:1:1 (w/w/w)	inkjet and aerosol-jet printing	3.23	microelectrode arrays (MEAs) and biomedical devices	[12]
PPy	polycaprolactone (PPy-b-PCL)	in-house built EHD-jet AM (electrohydrodynamic)	0.12	nerve guide conduits	[160]

metallic nanoparticles within a polymer matrix can be applied to improve its electrical properties without drastically changing the bulk material; it therefore can be used in AM via a variety of technologies, such as FDM, DIW, SLA, inkjet, etc. For example, Mannoor et al. coupled nanoelectronics with biological systems when making their AM printed ear, as shown in Fig. 5a [124]. The ear was printed via DIW, and the ink consisted of a chondrocyte-seeded alginate hydrogel matrix with a conductive silver nanoparticle-infused inductive coil antenna. The ear was able to receive electromagnetic signals over a wide range of frequencies (Hz-GHz). Lei et al. also demonstrated the possibilities of AM silver/-polymer composites through printing conductive circuits using silver/PVB filaments via FDM [125]. At 55 wt% loading of the silver powder, a low resistivity of 7.02×10^{-4} Ω cm was obtained. The composite material also showed improved microhardness (31.90 $HV_{0.2}$) compared to PLA-only filaments (23.37 $HV_{0.2}$), with their results showing promising applications in PCB, RFID, and electronic paper.

Tan and co-workers developed a conductive filament for FFF comprised of nickel and $Sn_{95}Ag_4Cu_1$ (5–35 vol%) alloy in a nylon–6 or polyethylene (PE) thermoplastic matrix [129]. The percolation threshold for electrical conductivity of the alloy composites was found to be ~25 vol% for both polymers. At 30 vol% in a Nylon-6 matrix, the electrical conductivity was $> 31{,}000$ S m^{-1} and 23,000 S m^{-1} for the PE matrix at a loading of 35 vol%. The conductive filament also showed changes in mechanical properties compared to the neat polymer. Both Young's moduli and the ultimate tensile strength (UTS) increased with greater solid loading of the alloy in Nylon-6, but a decrease in toughness was observed. A similar result was obtained when printing using the PE matrix, except the UTS started to decrease after loadings greater than 20 vol%. This effect is commonly seen in the AM of composites using filler materials, as there is often a trade-off between electrical conductivity and the mechanical properties of the composite. Specifically, although an increase in metallic filler concentration will lead to high electrical conductivity in the composite, it can also lead to brittleness, limiting the applications of the printed part. Yung et al. took a different approach to the AM of a thermoplastic (PLA) via FFF by applying a photochemical coating of copper [126]. Acrylic paint containing malachite (5:2 malachite to acrylic mass ratio) was painted onto the additive manufactured structures to form a copper coating after laser treatment. The recorded resistance of the coated additive manufactured object was 4.3×10^{-7} Ωm. Yung et al. demonstrated the potential of this method by using laser writing to photochemically reduce conductive copper tracks on the coating, which could be used to light an LED on an additive manufactured hand (Fig. 5b).

5.2. Carbon-based nanomaterials

Carbon materials have been a key focus filler material for many polymer composites due to carbon's relatively high electrical conductivity [130], light weight, and low cost. A wide range of carbon nanomaterials are available to be explored, such as carbon black [131,132], graphite [133], graphene, graphene oxide [134,135], carbon nanotubes [136], and carbon nanofibers [137].

5.2.1. Carbon black

Carbon black is one of the most abundantly used nanomaterials for polymer composites due to its good electrical conductivity and

Table 3
Electrical properties of additive manufactured printed conductive fillers in polymer composites.

Conductive Filler	Loading of Filler	Polymer Matrix	Additive Manufacturing Technology	Electrical Properties	Applications	Ref.
carbon black	32.3 wt%	polypropylene	FDM	< 1000−200 Ω cm	AM sensors	[139]
graphene	10 wt%	PMMA and PPy (10 wt %)	FDM	14.2 S cm^{-1}	alternative to wiring or expensive printable conductive inks	[150]
silver	55 wt%	polyvinyl butyral (PVB)	FDM	7.02×10^{-4} Ω cm	PCB, RFID, and electronic paper	[125]
nickel particles (dispersed with $Sn_{95}Ag_4Cu_1$)	30 vol%	nylon-6	FFF	3.10×10^{2} S cm^{-1}	AM conductive tracks	[129]
multiwalled carbon nanotubes	30 wt%	PLA	DIW	23 S cm^{-1}	sensors (gas or strain sensors) and EMI shielding	[177]
nano-carbon black (CB)	4 wt%	polyamide 12	SLS	7.71×10^{-5} S cm^{-1}	conductive polymer composites for SLS printing	[193]
carbon black	4 wt%	nylon-12	SLS	1.00×10^{-4} S cm^{-1}	conductive polymer composites for SLS printing	[194]
CNTs	0.3 wt%	methyl ether methacrylate (PEGMEMA)	DLP	8.00×10^{-6} S cm^{-1}	3D structures with conductive electrical properties	[195]
silver nanoparticles	20 wt%	PEGDA	SLA	1.50×10^{5} Ω cm	composite metal-polymer 3D structures	[81]
CNTs	0.5 wt%	polyurethane (PU)	DIW	1.00×10^{-6} S cm^{-1}	MEMS, electromagnetic shielding meshes, flexible electronic connections	[196]
graphene	75 wt%	polylactide-co-glycolide	DIW	~6.5 S cm^{-1}	medicine, bioelectronics, sensors, and energy devices	[162]
reduced graphene oxide (rGO)	5.6 wt%	ABS	DIW	1.05×10^{-5} S cm^{-1}	AM of electrically conductive materials	[151]
CNT	10 wt%	PLA	FDM	~1 S cm^{-1}	manufacturing of structural and conductive components	[197]
GNP	15 wt%	ABS	FDM	10^{-8}–10^{-5} S m^{-1}	AM of electrically conductive materials	[198]
graphene oxide	0.5 wt%	PEGDA	DLP	4.08×10^{-9} S cm^{-1}	graphene-based 3D-printed composite	[199]
silver	–	UV-cured polymer	inkjet	1.00×10^{4} S cm^{-1}	AM antennas	[200]
CNTs	~0.49 wt%	PBT polybutylene terephthalate	FDM	~0.01 S cm^{-1}	manufacturing of functional structures	[148]
CNTs	~3 vol %	HDPE	FFF	$\sim 10^{-2}$ S cm^{-1}	designing electro-conductive polymer nanocomposites (PNCs)	[147]
MWCNTs	5 wt%	TPU	FDM	$\sim 1.00 \times 10^{-2}$ S cm^{-1}	piezoresistive feedstock for AM of strain sensors	[201]
MWCNTs	0.3 wt%	commercial acrylic-based photocurable resin	DLP	2.70×10^{-4} S m^{-1}	hollow capacitive sensors, smart structures with shape memory effects, and stretchable spring circuits	[202]

reinforcing properties for polymers and elastomers [138], so it presents as a good choice for the AM of conductive nanocomposites. Conductive nanocomposites incorporating carbon black have been reported by Kwok et al., who developed a conductive polypropylene filament for FFF [139]. Carbon black particles (15.5, 25.9, 32.3 wt%) were blended with PP in a single-screw extruder, producing an electrically conductive polymer composite filament. The AM filament achieved electrical resistivity below 10^{-2} Ω m with concentrations greater than 30 wt% and a percolation threshold of ~11.3 wt%. Kwok et al. demonstrated the capability of their filament by additive manufacturing circuits powered with a 9 V battery to light a blue LED. Similarly, the use of carbon black for FFF printing has been described, but in this work, a commercially available carbon black-based FFF filament (Palmiga PI–ETPU) was used to print a metamaterial for a capacitive sensing array for human joint wearables [140]. Espera Jr et al. reported the use of carbon black powders with polyamide-12 for SLS applications [141]. Through varying the percentage of carbon black (0, 1.5, 3, 5, and 10 wt%) in PA12 powder, the electrical conductivity of the nanocomposites was studied. The percolation threshold was reported to be between 1.5 and 3 wt% carbon black concentration, with the highest electrical conductivity reported as 11.17 μS cm^{-1} for the composite containing 10 wt% carbon black.

Affordable AM of carbon black polymer nanocomposites has been reported by João et al., who demonstrated the fabrication of an electrochemical sensor using a cheap AM pen and a commercially available conductive filament (Proto-Pasta®, obtained from ProtoPlant Inc., Vancouver, Canada) [142]. AM pens use a filament that is extruded through a heated nozzle powered by a battery usually associated with a children's toy. However, João et al. reported that their pen AM electrode could detect lead and copper in tap water and liquid fuels (both 100 μg L^{-1}), which could provide a cheap and portable solution for field analysis. Undoubtedly, the availability and good processing properties of carbon black offer a good option for AM, resulting in interesting applications that include stretchable conductors [143], electrochemical sensors [142], health monitoring devices [144], smart textiles [145], and microwave absorption materials [146].

5.2.2. *Carbon nanotubes*

Carbon nanotubes — cylindrical particles made of one or several concentric graphite layers — have been used as additives in many AM applications to produce conductive polymer nanocomposites. Recent work demonstrated the conductivity of FFF CNTs using PLA and HDPE as the polymer matrix [147]. Filaments containing CNTs were prepared and mixed with the polymers using melt-mixing processes with a twin extruder. The loading of the CNTs was 0, 0.5, 0.5, 1, 2, 4, and 6 as a percentage of weight fraction to the polymer. The measured data found the percolation threshold for the composites to be 0.23 vol% for

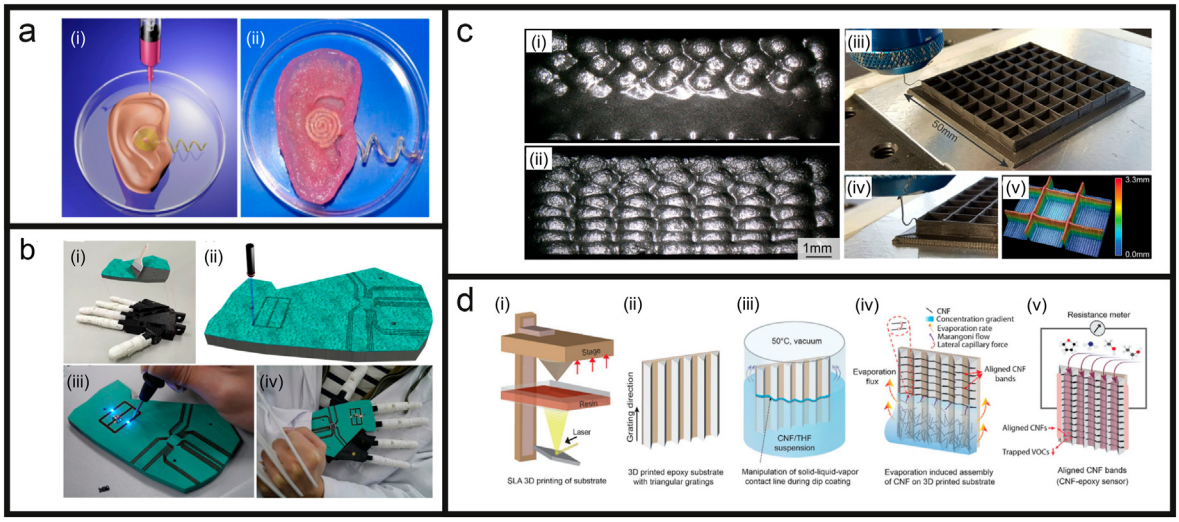

Fig. 5. (a) Illustration of a bionic ear (i) and optical image of an AM ear (ii) (Copyright© The American Chemical Society: [124]). (b) Image of AM robot hand being brushed by acrylic paint containing malachite (i); schematic showing laser writing technique to pattern circuit tracks (ii); testing of the tracks using LED lightbulb (iii); image of the robot hand in use, showing powered red LEDs (iv) (Copyright© Sci. Rep. 2016: [126]). (c) Optical microscope images showing the surface of printed 20 wt% graphene in epoxy (i) and 20 wt% graphene + clay in epoxy (ii); a photograph of the DIW printing process using 20 wt% graphene + clay formulation (iii, iv); height map of the printed wafer tray, showing minimal height variations (v) (Copyright© Elsevier, 2018: [126,127]). (d) Schematic showing: SLA printing process (i), AM epoxy with triangular gratings for nanoparticle patterning (ii), dip-coating process (iii), mechanism of CNF band formation (iv); and a CNF-epoxy composite as a sensor device (v) (Copyright© The Royal Society of Chemistry, 2020: [128]).

CNT/PLA and 0.18 vol% for the CNT/HDPE polymer. Gnanasekaran et al. compared the printability and properties of their CNT/polybutylene terephthalate (PBT) FFF filaments with graphene (G/PBT) FFF filament [148]. Both melt-extruded composites were printed using an Ultimaker 2 desktop printer. Gnanasekaran et al. reported their G/PBT printed filaments appeared rough and brittle in comparison to the CNT/PBT printed filaments, suggesting that the overall quality [149] of the printed material was superior in the composites containing CNTs. The CNT/PBT printed composites in this study also showed superior electrical properties, with a percolation threshold of ~0.49 wt% of CNT (~0.31 vol%), compared to the much higher quantities needed for the G/PBT based composite, at ~5.2 wt% (~ 3.3 vol%). Both composite filaments in this study provided a low-cost solution for the additive manufacturing of electrically conductive materials [148].

A novel approach with AM MWCNTs was reported by Chavez et al., who described the in situ alignment of a conductive filler within a photopolymer via applied electric fields [149]. This method enabled the properties of the printed polymer nanocomposite to be finely tuned to control not only the electrical properties of the SLA printed part but also the mechanical properties. Through adjusting the frequency and electric field, the orientation of the printed component while printing the MWCNTs could be aligned randomly, in parallel, and perpendicularly. The results indicated an improvement in UTS for both samples when their fillers were aligned in parallel or perpendicular to the test directions. Critically, the electrical conductivity of the samples where the MWCNTs were aligned in parallel showed an improvement of 89.3%. However, when the fillers were aligned perpendicular to the test electrodes, the conductivity was around 6 times lower than that of the parallel samples. This work highlights the ability to improve the electrical properties of AM polymers using conductive filler materials; it also shows that aligning these fillers enables the fine-tuning of electrical properties as well as thermal and mechanical properties.

5.2.3. Graphene

Graphene is a 2D material has reported to their unique optical, electrical, and physicochemical properties and has gained significant attention as a conductive filler material for AM due to its reported beneficial properties. The development of graphene-based polymer nanocomposites can provide conductive materials for a variety of applications from electrochemical sensors to biological implants. Mohan and co-workers [150] added a 10% graphene content to a hybrid polymer consisting of the primary polymer (PMMA) and secondary polymer polypyrrole (PPy, 10%). Conductive filaments for FDM applications were prepared and printed achieving high electrical conductivities of 14.2 S cm^{-1}. Similarly, Foster et al. used commercially available graphene/PLA filament that could be AM via FFF for energy storage devices [1,3]. Here, additive manufactured disk electrodes were printed out of commercially available conductive filament for freestanding lithium-ion anodes in a Li-Ion coin cell. FDM printed graphene-based polymer composite was also demonstrated by Wei et al. to improve the electrical conductivity of ABS [151]. With the addition of 5.6 wt% loading of graphene in ABS the printed composites achieved a conductivity of 1.05×10^{-3} S $m^{-1}$and a percolation threshold calculated to be ~2 wt%. Meanwhile, other work took a different approach in the fabrication of graphene-reinforced epoxy printed via DIW methods [152]. The bulk resistivity of the printed epoxy-graphene (20 wt%) along the print direction was significantly lower than the resistivity of epoxy alone (Fig. 5c). Hensleigh et al. reported the AM of their XGO resin containing graphene oxide (GO) and a UV-curable acrylate resin for projection micro-stereolithography (PμSL) applications [153]. Although their main aim was to produce micro-architected graphene (MAG) by reducing the GO to rGO and subsequently removing the acrylate polymer, this work demonstrated the ability to AM graphene-polymer composites via laser-based AM techniques for potential use in electrically conductive UV-curable resins.

5.2.4. Carbon nanofibers

Carbon nanofibers, an analog of carbon, can be used as conductive fillers in polymer composites to improve the electrical conductivities of 3D printable polymers. Much like all conductive fillers used in polymer composites, carbon nanofibers rely on good dispersions in the polymer matrix to create continuous conductive pathways for electrical conductivity [154]. Rymansaib et al. incorporated carbon nanofibers with graphite in polystyrene (HIPs) to produce electrically conductive filaments for FFF [5]. Conductive filaments comprised of 80 wt% polystyrene, 10 wt% carbon nanofibers, and 10 wt% graphite flakes and were used to print electrodes for voltammetric sensing and detecting heavy metals. The group also reported the detection of Pb on the surface of the composite electrode, highlighting the potential for AM conductive

polymer nanocomposites for applications in health-related sensors and the monitoring of metal pollutants.

Jambhulkar and co-workers took a different approach to developing an AM conductive CNF–epoxy polymer composite via SLA [128]. The group conducted AM upon an epoxy-patterned substrate via SLA and then subsequently dip-coated the substrate into a CNF/THF solution, which resulted in the assembly of CNFs on the substrate upon evaporation of the THF. The ability to 3D print small channels with a spacing of 200 μm allowed for conductive sensing components, as the CNFs were able to align directionally along the channels for improved directional conductivity. The reported resistance for the composites containing 0.1, 0.5, 1.0, and 10.0 mg ml^{-1} CNF/THF was 1.4, 2.1, and 16.3 kΩ, respectively. The conductive nanocomposite was then successfully used to print chemical sensors that could detect volatile organic compounds (VOCs), see Fig. 5d.

In summary, comparisons of metallic and carbon fillers have shown that metallic fillers have considerably higher conductivity but clearly also have higher costs, so research continues to explore the effect of carbon fillers.

6. Applications of AM conductive polymers and polymer nanocomposites

Multifunctional AM CPs and polymer nanocomposites offer opportunities in a myriad of applications, from tissue engineering to soft robotic actuators [155] and even organic dual-band antennas [156]. The literature of AM CPs and polymer nanocomposites mainly focuses on four key areas: bioelectronics; flexible and stretchable electronics; sensors; and electrochemical devices. The achievements in each field are discussed in the following sub-sections.

6.1. Bioelectronics

There is no doubt that many of the published studies about AM CPs are related to applications in the biomedical field, from drug delivery systems [157] to sensors for orthopedic implants [158]. One key area being explored is tissue engineering, where, for example, Heo et al. reported an AM conductive PEDOT:PSS/PEGDA hydrogel printed via SLA [159]. The reported hydrogel showed significant improvement in the electrical potential for neuronal differentiation. The mechanical properties of the hydrogel showed a decrease in compressive stiffness with increasing concentration of PEDOT:PSS from 35.4 ± 1.4 MPa (0 wt%) to 26.3 ± 4.2 MPa (0.9 wt%). The reported cell viability results showed that with increasing amounts of PEDOT:PSS in the hydrogel there was a slight positive effect on the cellular behavior, with an increase in the number of cells that showed no observable cytotoxic effects (Fig. 6a).

Vijayavenkataraman et al. reported the AM of a biodegradable and conductive copolymer of PPy and polycaprolactone (PPy-b-PCL) for porous nerve guide conduits (NGCs) intended for peripheral nerve injury repair [160]. Increasing concentrations of 1–2 v/v% PPy-b-PCL were printed via an electrohydrodynamic-jetting (EHD-jet) printer [165]. The electrical and mechanical properties and cell viability were explored to examine the suitability of the printed composite for application. Vijayavenkataraman et al. found that increasing the concentration of PPy-b-PCL reduced the mechanical properties, meaning the structures became softer to imitate the properties of the native human peripheral nerve. As expected, the conductivity of the composites increased as the concentration of the conductive component PPy was raised from 0.28 ± 0.02 mS cm^{-1} (PCL/PPy 0.5%) to 1.15 ± 0.03 mS cm^{-1} (PCL/PPy 2%). Observation of cell viability showed human embryonic stem cell-derived neural crest stem cells (hESC-NCSCs) attach and differentiate into peripheral neurons on the printed composite scaffolds. These results showed promise for AM conductive polymers for tissue-engineering applications.

Ma et al. explored the effects of the concentration and morphology of polypyrrole nanoparticles for tissue engineering scaffolds [66]. Both tubular (10 μm in length, outer diameter of 100–300 nm) and spherical

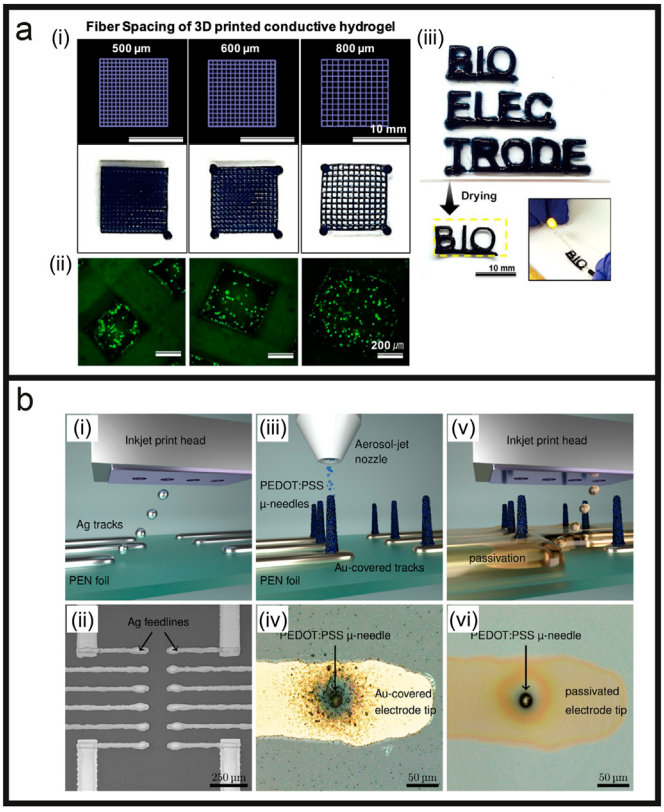

Fig. 6. (a) (i) (From top to bottom) CAD drawing of a scaffold with varying square widths (width = 500, 600, and 800 μm); AM pattern of PEDOT/PSS hydrogel; (ii) encapsulated DRG cells in GelMa. (iii) Optical images of AM PEDOT:PSS hydrogel displaying drying effects, and a photograph of dried hydrogel connected to an LED (Copyright© Elsevier, 2019: [159]). (b) 3D fabrication process of μ-needle electrode arrays. (Copyright© The American Chemical Society, 2019 [12]).

(50 nm diameter) particles were dispersed in a poly-l-lactide (PLLA) matrix and fabricated via DIW. Ma et al. found that at the same concentration, tubular PPy displayed a higher conductivity for the AM parts (~2 × 10^{-5} S cm^{-1}) than spherical PPy (~7.5 × 10^{-5} S cm^{-1}). The composites were recorded to be cytocompatible for applications in tissue engineering scaffolds. Weng et al. also explored the application of CPs in tissue engineering using a PPy/collagen composite printed using an inkjet [161]. The composite material was printed on a polyarylate for cell patterning purposes and achieved an electrical conductivity of 1.1 S cm^{-1}. In vitro cell study tests confirmed the material's suitability for tissue engineering applications, as more than 90% of the cells adhered to the PPy/collagen printed pattern.

Meanwhile, Zips et al. took a different approach and reported their additive manufactured PEDOT:PSS-MWCNT composites for bioelectronics applications (Fig. 6b) [12]. They used a combination of inkjet and aerosol printing to fabricate needle-like electrode tips (μ-needles) with a diameter of 10 ± 2 μm and a height of 33 ± 4 μm. The electrical performance tests exhibited a conductivity of 323 ± 75 S m^{-1} and a capacitance of 242 ± 70 nF at a scan rate of 5 mV s^{-1} and an impedance of 128 ± 22 kΩ at 1 kHz frequency. They tested their fabricated μ-needle microelectrode arrays (MEAs) using cell-culture compatibility tests with cardiomyocyte-like HL-1 cells and established their relevance for electrophysiological recordings from living cells.

AM graphene-based polymer composites for biomedical applications were reported by Jakus et al., with their liquid ink consisting of polylactide-co-glycolide (a biomedical polymer) and graphene [162]. The conductive ink was printed via DIW methods that produced robust structures with a reported electrical conductivity of over 800 S m^{-1}. The

addition of graphene in the composite ink was used to enhance cell–cell signaling, cell differentiation, and cell function, which were subsequently assessed by seeding female bone-marrow-derived human mesenchymal stem cells (hMSCs) onto AM scaffolds containing 60 vol% graphene. The results demonstrated that the hMSCs were viable on the printed scaffolds for 2 weeks and proliferated to coat the scaffold, showing promise for bioelectronic medical devices.

6.2. Flexible and stretchable electronics

Flexible and stretchable electronics is a growing field for new wearable technologies that are lightweight and can perform under considerable amounts of strain without failure [163,164]. These innovative materials can be applied as electronic skins, stretchable transistors, sensors, and supercapacitors. As CPs aren't inherently flexible or stretchable to the extent needed for flexible and stretchable electronics, they are often blended with a second polymer, such as silicon or an elastomer, to enhance their mechanical properties and still maintain electrical conductivity [165,166].

Teo and co-workers reported printing a PEDOT:PSS/ionic liquid hydrogel composite via microreactive inkjet printing (MRIJP) that could be applied for wearable and stretchable electronic device purposes [13]. The composite achieved conductivities of 900 S cm^{-1} with a resolution of ≈60 μm (drop diameter). Vaithilingam et al. reported inkjet printing PEDOT:PSS onto a flexible and stretchable substrate that could be used in flexible electronic applications [167]. The group printed conductive PEDOT:PSS tracks onto a commercial resin TangoBlack® FLX973 substrate. The printed composite was able to withstand extensions of up to 3 mm before cracking, and it contracted back to its original shape. The resistance was tested before (1–2 KΩ) and after (10–15 KΩ) elongation, showing an increase in resistance after stretching. The printed composite could also be flexed with a resistance of (1.1–2.1 KΩ) up to a radius of curvature of 15 mm before cracking.

Some researchers have taken a different approach to incorporating CPs and AM without directly printing the CP. Instead, they have fabricated the CPs via coatings or infiltration of the conductive polymer onto the printed material. Hoffman et al. demonstrated this by blending an AM Nafion® template and ABS (30 wt%) via FFF and then submerging the polymerized part in an activation bath of PEDOT (Fig. 7a) [168]. This technique allowed conductive PEDOT to polymerize with the Nafion® template to achieve a bulk conductivity of 3 S cm^{-1}, permitting the fabrication of conductive flexible parts for organic electrochemical transistor (OECT) devices and wearable electronics, e-textiles, and biosensors. Li et al. fabricated highly stretchable micro-supercapacitors using a combination of AM and coating techniques [169]. To fabricate the micro-supercapacitors, a template was additive manufactured using DIW; PDMS was then cast on it to obtain a stretchable substrate with wavy tracks onto which a slurry of PANI nanorods-coated MWCNTs was injected as an electrode. The electrode yielded a specific capacitance of 44.13 mF cm^{-2} and a capacitance retention of 87% after 20,000 cycles. The fabricated structures maintained this stability even after stretching, twisting, crimping, and winding of the electrode (Fig. 7 b).

Both Duan et al. [170] and Zhang et al. [171] reported the use of AM conductive graphene networks in highly stretchable and flexible polymers for next-generation electronics. Duan et al. reported the use of extrusion-based printing to form a porous PLA network that was infiltrated with PDMS integrated with carbon nanotubes and graphene [170]. Their AM highly stretchable polymer composite displayed electrical stability over a 5,000-bend cycle and showed minimal decrease in electrical conductivity over 100 stretching cycles under 50% strain, indicating great promise for future stretchable electronics. Zhang et al. melt-blended PLA with graphene to form conductive (4.76 S cm^{-1} at 6 wt % graphene) and flexible filaments for FDM applications, which showed promise in the organic electronics field [171].

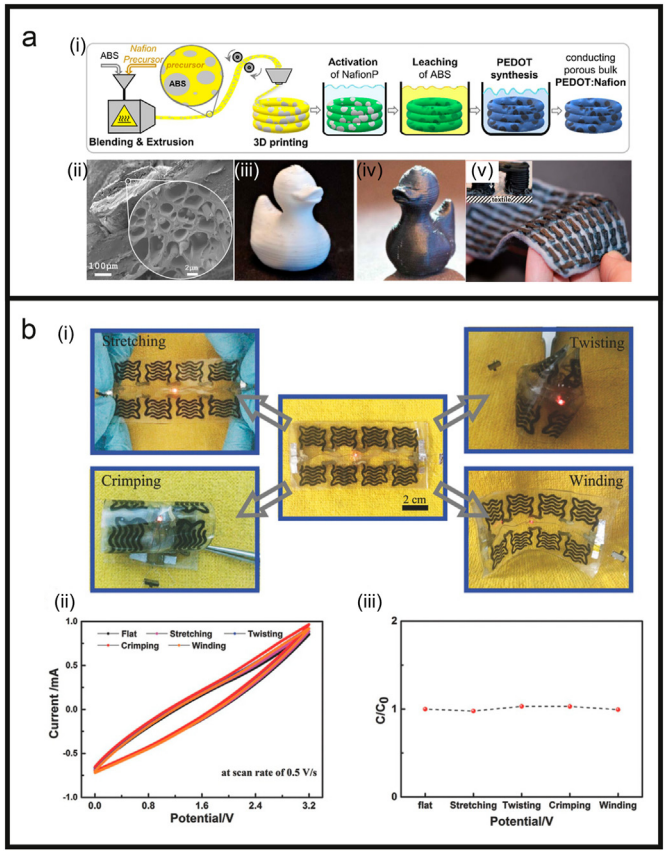

Fig. 7. (a) (i) Schematic of processing precursor/ABS blends via FFF to obtain PEDOT:Nafion® structures. (ii) SEM image of the cross-section of an AM line of Nafion®/ABS with a 30 μm coating of PEDOT:Nafion®. FFF printed duck of Nafion®/ABS before (iii) and after PEDOT synthesis (iv). (v) 100-leg thermoelectric module (Copyright© The American Chemical Society, 2020: [168]). (b) (i) Optical images of a stretchable micro-supercapacitor undergoing deformation (stretching, twisting, crimping, and winding), showing it lighting a red LED. (ii) CV curves under various types of deformations at a scan rate of 0.5 V s^{-1} (iii) Normalized capacitance (C/C 0) of the device under different deformations (Copyright© Wiley, 2017: [169]).

6.3. Sensors

The use of conductive polymers in sensing applications has been widely reported in the literature [34,172,173]. CPs can be applied as sensitive layers because of their high sensitivities, low production costs, and ability to detect considerable amounts of volatile substances. Devaraj et al. demonstrated the AM of the conductive polymer PEDOT:PSS for digital airflow sensor applications [174]. Micro-hair structures made from PEDOT:PSS were printed via FFF, to imitate natural fluid airflow sensors (hairs) (Fig. 8a). An array of the micro-hair sensors acted as switches to a common terminal in response to airflow. The printed sensor was capable of measuring flow from 61 to 91 mm s^{-1}, due to its excellent electrical and mechanical properties. In another example, Tarabella et al. demonstrated the use of PEDOT:PSS for resistive humidity sensors. In this case, PEDOT:PSS was used as a coating on top of an SLS-printed polyamide structure used as a template [175].

Cullen and co-workers described the AM of PPy composites via DLP for potential uses in sensing applications [9]. PPy was blended with urethane dimethylacrylate (UDMA) to improve the mechanical properties of the composite, due to polypyrrole's brittle nature. The UDMA also aided in the 3D process but hindered the overall conductivity (Fig. 8b). Although no specific sensing tests were verified in this work, the authors

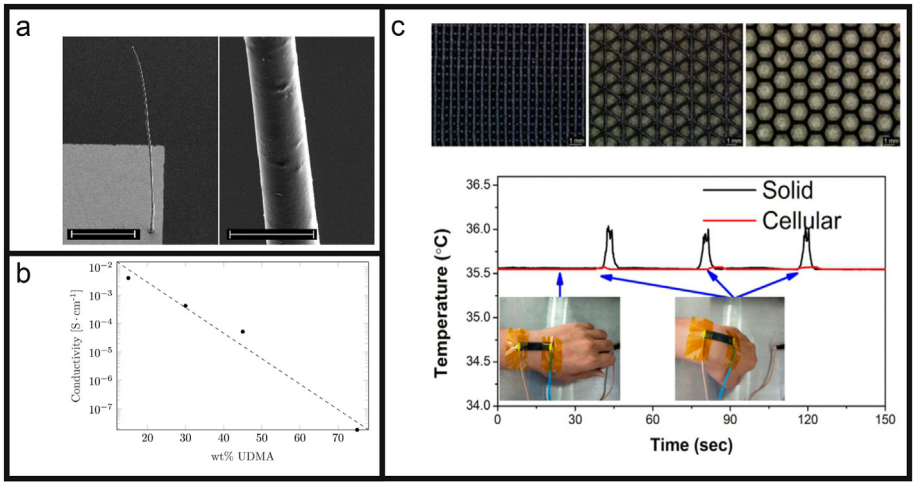

Fig. 8. (a) SEM of 1000 μm long micro-hair structure (scale bar 200 μm) (left), and the surface of a PEDOT:PSS micro-hair (scale bar 10 μm) (right) (Copyright© IEEE, 2015: [174]). (b) Electrical conductivity of CP composite versus weight fraction of UDMA (Copyright© Elsevier, 2018: [9]). (c) (above) Optic images showing AM graphene/PDMS with a grid structure, triangular porous structure, and hexagonal porous structure (left to right); (below) monitoring of skin temperature and joint bending using the AM sensor (Copyright© American Chemical Society, 2019: [176]).

suggested this technique and conductive material would be suitable for sensing applications in the future. Similarly, Benjamin-Holness et al. reported an AM PANI-based composite for potential sensing applications [10]. PANI was printed via a DIW technique, but this provided a minimum feature size of 1.5 mm, which was a much larger resolution than previously described AM CPs [106]. To enhance the conductivity of the printed material, PANI was doped with DBSA and heated during the post-processing stage for thermal doping purposes. The ideal thermal doping parameters were found to be 145 °C for 10 min, which boosted the electrical conductivity from 0.2 to 3.26 S cm^{-1} before and after doping, respectively. Although specific sensing applications were not tested in this work, the material and fabrication method show promise for the future development of CP sensors printed using DIW.

Wang et al. developed a stretchable temperature sensor consisting of graphene and PDMS [176]. In this work, the group optimized the sensing capabilities by adapting the structural designs printed using DIW to include grid, triangular, and hexagonal structures (Fig. 8c). As many conductive nanocomposites suffer from strain-sensitive effects, the variations in these printing structures compensate for these effects to improve the sensing capabilities under external deformation. The performance of the printed grid structure showed a good stretchability of 50–60% and a sensitivity decrease of ~15% under large tensile strain compared to a solid printed nanocomposite, which showed a stretchability of ~35% and a decrease in sensitivity of ~90%. The performance of the conductive nanocomposites in this work could be applied to wearable temperature sensors. Chizari et al. developed a liquid sensor consisting of CNTs and PLA, which could be printed via FDM [177]. In their work, the group also optimized the structural parameters to optimize the performance of the liquid sensor. They found that by varying the inter-filament spacing (IFS) from 0.2 to 1.5 mm, the average relative resistance change varied from ~78% to ~238%, respectively. The lowest sensitivity of 78% was attributed to the structure being compact with smaller IFS, meaning there was more inaccessible surface area, decreasing the effect of the liquid sensor. They also found that by reducing the filament diameter from 433 to 128 μm, the sensitivity increased from 58% to 290%, respectively. These works demonstrate that optimizing the printing parameters of conductive nanocomposites is important for their performance as sensors.

6.4. Electrochemical devices

The fabrication of electrochemical devices via AM offers the unique advantages of complex designs with high surface areas. CPs used in electrochemical devices have shown great promise due to good electrode interfaces between the electronic and ionic transporting phases [178,179]. CP polymer composites can be used to improve the overall processibilities of CPs for AM applications whilst maintaining functionality for electrochemical devices [180,181].

Wang et al. demonstrated the potential of a reduced graphene oxide (rGO)/PANI composite AM via DIW for electrochemical devices [44]. In this work, rGO sheets were used to form a 3D dynamic network with PANI chains assembling directly onto the GO sheets, driven by strong π–π interactions. The recorded areal specific capacitance of their AM device was 1255 ± 74 mF cm^{-2} (volumetric specific capacitance: 12.5 ± 0.8 F cm^{-3}) at a current density of 4.2 ± 0.8 mA cm^{-2} (Fig. 9a). These results showed potential for applications in supercapacitors and energy devices. Qi et al. also used DIW to print PPy/graphene electrodes for electrochemical energy storage; however, in this work, PPy was used to coat the AM graphene–aerogel structure rather than directly printing the PPy [182]. While the authors reported the benefit of the hierarchical porous printed structure's large specific surface area (786 m^2 g^{-1}), the deposition of the active material PPy was mainly focused on the outer surface rather than the small internal pores. Even so, the reported printed PPy/GA electrode showed an areal capacitance and energy density of 2 F cm^{-2} and 0.78 mWh cm^{-2}, respectively. Also, the porous lightweight structure of the printed aerogel allowed for enhanced compressibility and full recovery of the printed electrodes. This novel approach could be applied in batteries, solar cells, and fuel cells.

Lu et al. took a different approach and manufactured a porous iron-nickel/polyaniline nanocages supercapacitor via selective laser melting (SLM) [184]. Here, the Ni-based alloy was fabricated via AM to produce a porous architecture for energy storage; PANI was then deposited onto it via anodic electrochemical polymerization. The described specific capacitance results for the AM CP composite were 540.68, 390.25, 114.84, 84.20, 49.85, and 23.57 F g^{-1} at scan rates of 5, 10, 50, 100, 200, and 500 mV s^{-1}, respectively. Shim et al. reported an inkjet printed electrochromic device made out of a PANI/silica and PEDOT/silica composite [183]. An electrochromic device is an electrochemical cell that changes color when electric potential energy is applied. The colloidal suspension of the CPs in a solvent allowed the viscosity to remain low enough for inkjet printing of the active color-changing layer in the devices. Each inkjet printed device showed a color change when a voltage was applied, from −2 to +2 V for both PANI/silica and PEDOT/silica composites (Fig. 9b). The color change shown

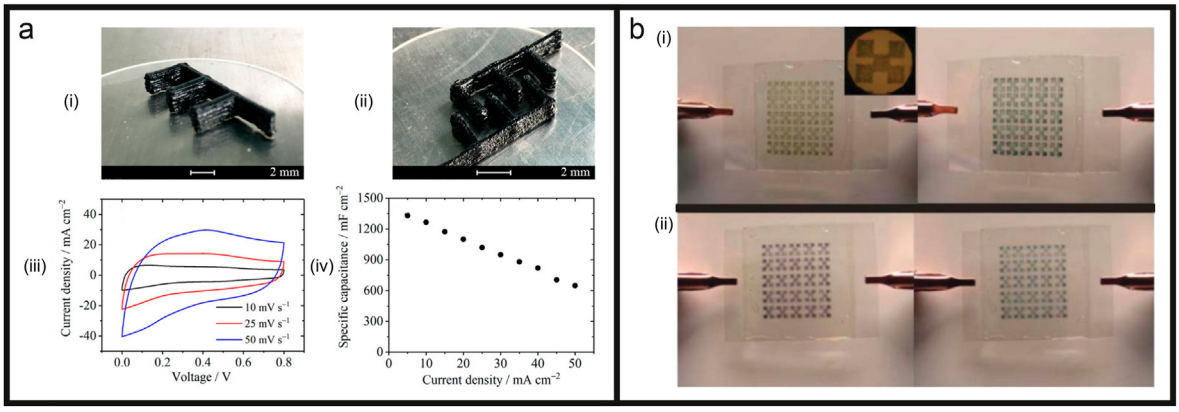

Fig. 9. (a) Photograph of DIW printed (rGO) (i)/PANI supercapacitor (ii). (iii) CV curves of the planar supercapacitor at various scan rates. (iv) Specific capacitances at various current densities (Copyright© ACS, 2018: [44]). (b) Inkjet printed electrochromic devices: (i) PANI-based ECD at −2 and + 2 V; (ii) a PEDOT-based ECD at −2 and + 2 V (Copyright© The Royal Society of Chemistry, 2008: [183]).

corresponded to the redox state of the CPs when the varied voltage was applied.

7. Conclusions and outlook

This review has presented an overview of the major achievements within the field of additively manufactured conductive polymers and nanocomposites, which allow the achievement of high electrical conductivities that can be applied in a myriad of applications, including bioelectronics, flexible and stretchable electronics, sensors, and electrochemical devices, to name just a few. The ability to additively manufacture conductive polymers and polymer nanocomposites allows for the fabrication of lightweight, conductive, and complex designs. This is an exciting prospect for the additive manufacturing industry, as multifunctional components can be manufactured, expanding the existing realms of additively manufactured polymers with limited functionality that have predominantly been applied in prototyping.

The main areas of debate in the additive manufacture of conductive polymers and nanocomposites include improving the stability and dispersion of nanoparticles in polymers to allow for uniform printing and better electrical conductivity. Another key consideration is the trade-off between the electrical conductivity of the printed materials and their mechanical properties, as high loadings of filler materials and CPs often lead to a reduction in mechanical properties due to their brittle nature. Incorporating a second polymer has shown promise for achieving the desired mechanical properties as well as decent conductivity, and we suggest this should receive particular emphasis in future studies.

The current literature demonstrates the high electrical conductivities that can be achieved through the printing of both CPs and polymer nanocomposites. However, it remains unclear whether additively manufactured conductive polymers and nanocomposites can truly compete against additively manufactured metal components. We anticipate that through the development of new hardware for additive manufacturing technologies, significant improvements to the electrical and mechanical properties of conductive polymers and nanocomposite can be anticipated.

Declaration of competing interest

The authors declare that they have no known competing financial interests or personal relationships that could have appeared to influence the work reported in this paper.

References

[1] C.W. Foster, M.P. Down, Y. Zhang, X. Ji, S.J. Rowley-Neale, G.C. Smith, P.J. Kelly, C.E. Banks, 3D printed graphene based energy storage devices, Sci. Rep. 7 (2017), 42233.
[2] E.M. Richter, D.P. Rocha, R.M. Cardoso, E.M. Keefe, C.W. Foster, R.A.A. Munoz, C.E. Banks, Complete additively manufactured (3D-printed) electrochemical sensing platform, Anal. Chem. 91 (2019) 12844–12851.
[3] M.P. Down, E. Martínez-Periñán, C.W. Foster, E. Lorenzo, G.C. Smith, C.E. Banks, Next-generation additive manufacturing of complete standalone sodium-ion energy storage architectures, Adv. Energy Mater. 9 (2019), 1803019.
[4] J. N, S. P, Application of 3D printed ABS based conductive carbon black composite sensor in void fraction measurement, Compos. B Eng. 159 (2019) 224–230.
[5] Z. Rymansaib, P. Iravani, E. Emslie, M. Medvidović-Kosanović, M. Sak-Bosnar, R. Verdejo, F. Marken, All-polystyrene 3D-printed electrochemical device with embedded carbon nanofiber-graphite-polystyrene composite conductor, Electroanalysis 28 (2016) 1517–1523.
[6] S.J. Rowley-Neale, D.A.C. Brownson, G.C. Smith, D.A.G. Sawtell, P.J. Kelly, C.E. Banks, 2D nanosheet molybdenum disulphide (MoS2) modified electrodes explored towards the hydrogen evolution reaction, Nanoscale 7 (2015) 18152–18168.
[7] E. Fantino, A. Chiappone, F. Calignano, M. Fontana, F. Pirri, I. Roppolo, In situ thermal generation of silver nanoparticles in 3D printed polymeric structures, Materials 9 (2016) 3712.
[8] G. Tarabella, S.L. Marasso, V. Bertana, D. Vurro, P. D'Angelo, S. Iannotta, M. Cocuzza, Multifunctional operation of an organic device with three-dimensional architecture, Materials 12 (2019) 1357.
[9] A.T. Cullen, A.D. Price, Digital light processing for the fabrication of 3D intrinsically conductive polymer structures, Synth. Met. 235 (2018) 34–41.
[10] F.B. Holness, D.P. Aaron, Robotic extrusion processes for direct ink writing of 3D conductive polyaniline structures, Proc. SPIE 9798 (2016) 124161426.
[11] V.B. Mohan, D. Bhattacharyya, Mechanical, electrical and thermal performance of hybrid polyethylene-graphene nanoplatelets-polypyrrole composites: a comparative analysis of 3D printed and compression molded samples, Polymer-Plastics Technol. Mater. 59 (2020) 780–796.
[12] S. Zips, L. Grob, P. Rinklin, K. Terkan, N.Y. Adly, L.J.K. Weiß, D. Mayer, B. Wolfrum, Fully printed μ-needle electrode array from conductive polymer ink for bioelectronic applications, ACS Appl. Mater. Interfaces 11 (2019) 32778–32786.
[13] M.Y. Teo, N. RaviChandran, N. Kim, S. Kee, L. Stuart, K.C. Aw, J. Stringer, Direct patterning of highly conductive PEDOT:PSS/ionic liquid hydrogel via microreactive inkjet printing, ACS Appl. Mater. Interfaces 11 (2019) 37069–37076.
[14] M.L. Griffith, J.W. Halloran, Scattering of ultraviolet radiation in turbid suspensions, J. Appl. Phys. 81 (1997) 2538–2546.
[15] U. Khan, A. O'Neill, H. Porwal, P. May, K. Nawaz, J.N. Coleman, Size selection of dispersed, exfoliated graphene flakes by controlled centrifugation, Carbon 50 (2012) 470–475.
[16] A. Harvey, C. Backes, J.B. Boland, X. He, A. Griffin, B. Szydlowska, C. Gabbett, J.F. Donegan, J.N. Coleman, Non-resonant light scattering in dispersions of 2D nanosheets, Nat. Commun. 9 (2018) 4553.
[17] C. Hinczewski, S. Corbel, T. Chartier, Ceramic suspensions suitable for stereolithography, J. Eur. Ceram. Soc. 18 (1998) 583–590.
[18] J. Jang, H.-G. Yi, D.-W. Cho, 3D printed tissue models: present and future, ACS Biomater. Sci. Eng. 2 (2016) 1722–1731.

[19] T. Abudula, R.O. Qurban, S.O. Bolarinwa, A.A. Mirza, M. Pasovic, A. Memic, 3D printing of metal/metal oxide incorporated thermoplastic nanocomposites with antimicrobial properties, Front. Bioeng. Biotechnol. 8 (2020) 568186.
[20] A. Ambrosi, M. Pumera, 3D-printing technologies for electrochemical applications, Chem. Soc. Rev. 45 (2016) 2740–2755.
[21] J. Bustillos, D. Montero-Zambrano, A. Loganathan, B. Boesl, A. Agarwal, Stereolithography-based 3D printed photosensitive polymer/boron nitride nanoplatelets composites, Polym. Compos. 40 (2019) 379–388.
[22] M.A. Alhnan, T.C. Okwuosa, M. Sadia, K.W. Wan, W. Ahmed, B. Arafat, Emergence of 3D printed dosage forms: opportunities and challenges, Pharm. Res. 33 (2016) 1817–1832.
[23] R.A. Barry Iii, R.F. Shepherd, J.N. Hanson, R.G. Nuzzo, P. Wiltzius, J.A. Lewis, Direct-write assembly of 3D hydrogel scaffolds for guided cell growth, Adv. Mat. 21 (2009) 2407–2410.
[24] J. Liao, H. Chen, H. Luo, X. Wang, K. Zhou, D. Zhang, Direct ink writing of zirconia three-dimensional structures, J. Mater. Chem. C 5 (2017) 5867–5871.
[25] D. Vernardou, K.C. Vasilopoulos, G. Kenanakis, 3D printed graphene-based electrodes with high electrochemical performance, Appl. Phys. A 123 (2017) 623.
[26] G. Hussain, W.A. Khan, H.A. Ashraf, H. Ahmad, H. Ahmed, A. Imran, I. Ahmad, K. Rehman, G. Abbas, Design and development of a lightweight SLS 3D printer with a controlled heating mechanism: Part A, Int. J. Lightweight Mater. Manufac. 2 (2019) 373–378.
[27] Z. Chen, Z. Li, J. Li, C. Liu, C. Lao, Y. Fu, C. Liu, Y. Li, P. Wang, Y. He, 3D printing of ceramics: a review, J. Eur. Ceram. Soc. 39 (2019) 661–687.
[28] B. Msallem, N. Sharma, S. Cao, F.S. Halbeisen, H.-F. Zeilhofer, F.M. Thieringer, Evaluation of the dimensional accuracy of 3D-printed anatomical mandibular models using FFF, SLA, SLS, MJ, and BJ printing technology, J. Clin. Med. 9 (2020) 817.
[29] M.A. Khan, E. Cantù, S. Tonello, M. Serpelloni, N.F. Lopomo, E. Sardini, A review on biomaterials for 3D conductive scaffolds for stimulating and monitoring cellular activities, Appl. Sci. 9 (2019) 961.
[30] J. Jagur-Grodzinski, Electronically conductive polymers, Polym. Adv. Technol. 13 (2002) 615–625.
[31] P.-O. Morin, T. Bura, M. Leclerc, Realizing the full potential of conjugated polymers: innovation in polymer synthesis, Mater. Horizons 3 (2016) 11–20.
[32] C.K. Chiang, C.R. Fincher, Y.W. Park, A.J. Heeger, H. Shirakawa, E.J. Louis, S.C. Gau, A.G. MacDiarmid, Electrical conductivity in doped polyacetylene, Phys. Rev. Lett. 39 (1977) 1098–1101.
[33] R. Balint, N.J. Cassidy, S.H. Cartmell, Conductive polymers: towards a smart biomaterial for tissue engineering, Acta Biomater. 10 (2014) 2341–2353.
[34] H. Bai, G. Shi, Gas sensors based on conducting polymers, Sensors 7 (2007) 267–307.
[35] S. Bhadra, N.K. Singha, D. Khastgir, Dielectric properties and EMI shielding efficiency of polyaniline and ethylene 1-octene based semi-conducting composites, Curr. Appl. Phys. 9 (2009) 396–403.
[36] Z. Gu, Y. Tan, K. Tsuchiya, T. Shimomura, K. Ogino, Synthesis and characterization of poly(3-hexylthiophene)-b-polystyrene for photovoltaic application, Polymers 3 (2011) 558–570.
[37] G.A. Snook, P. Kao, A.S. Best, Conducting-polymer-based supercapacitor devices and electrodes, J. Power Sources 196 (2011) 1–12.
[38] Y.J. Wang, G. Yu, Conjugated polymers: from synthesis, transport properties, to device applications, J. Polym. Sci. B Polym. Phys. 57 (2019) 1557–1558.
[39] M.T. Ramesan, K. Suhailath, 13 - role of nanoparticles on polymer composites, in: R.K. Mishra, S. Thomas, N. Kalarikkal (Eds.), Micro and Nano Fibrillar Composites (MFCs and NFCs) from Polymer Blends, Woodhead Publishing, 2017, pp. 301–326.
[40] Introduction of conducting polymers, in: M. Wan (Ed.), Conducting Polymers with Micro or Nanometer Structure, Springer Berlin Heidelberg, Berlin, Heidelberg, 2008, pp. 1–15.
[41] D. Kumar, R.C. Sharma, Advances in conductive polymers, Eur. Polym. J. 34 (1998) 1053–1060.
[42] E.M. Geniès, A. Boyle, M. Lapkowski, C. Tsintavis, Polyaniline: a historical survey, Synth. Met. 36 (1990) 139–182.
[43] S. Bhadra, N.K. Singha, D. Khastgir, Electrochemical synthesis of polyaniline and its comparison with chemically synthesized polyaniline, J. Appl. Polym. Sci. 104 (2007) 1900–1904.
[44] Z. Wang, Q.e. Zhang, S. Long, Y. Luo, P. Yu, Z. Tan, J. Bai, B. Qu, Y. Yang, J. Shi, H. Zhou, Z.-Y. Xiao, W. Hong, H. Bai, Three-dimensional printing of polyaniline/reduced graphene oxide composite for high-performance planar supercapacitor, ACS Appl. Mater. Interfaces 10 (2018) 10437–10444.
[45] F.B. Holness, A. Price, Robotic Extrusion Processes for Direct Ink Writing of 3D Conductive Polyaniline Structures, SPIE, 2016.
[46] N. Ferrer-Anglada, M. Kaempgen, S. Roth, Transparent and flexible carbon nanotube/polypyrrole and carbon nanotube/polyaniline pH sensors, physica status solidi (b) 243 (2006) 3519–3523.
[47] S. Bocchini, A. Chiolerio, S. Porro, D. Accardo, N. Garino, K. Bejtka, D. Perrone, C.F. Pirri, Synthesis of polyaniline-based inks, doping thereof and test device printing towards electronic applications, J. Mater. Chem. C 1 (2013) 5101–5109.
[48] A.G. MacDiarmid, L.S. Yang, W.-S. Huang, B.D. Humphrey, Polyaniline, Electrochemistry and application to rechargeable batteries, Synth. Met. 18 (1987) 393–398.
[49] M. Mitra, C. Kulsi, K. Chatterjee, K. Kargupta, S. Ganguly, D. Banerjee, S. Goswami, Reduced graphene oxide-polyaniline composites—synthesis, characterization and optimization for thermoelectric applications, RSC Adv. 5 (2015) 31039–31048.
[50] E.N. Zare, P. Makvandi, B. Ashtari, F. Rossi, A. Motahari, G. Perale, Progress in conductive polyaniline-based nanocomposites for biomedical applications: a review, J. Med. Chem. 63 (2020) 1–22.
[51] C.-H. Chang, T.-C. Huang, C.-W. Peng, T.-C. Yeh, H.-I. Lu, W.-I. Hung, C.-J. Weng, T.-I. Yang, J.-M. Yeh, Novel anticorrosion coatings prepared from polyaniline/graphene composites, Carbon 50 (2012) 5044–5051.
[52] Y. Yang, A.J. Heeger, Polyaniline as a transparent electrode for polymer light-emitting diodes: lower operating voltage and higher efficiency, Appl. Phys. Lett. 64 (1994) 1245–1247.
[53] D. Coltevieille, A. Le Méhauté, C. Challioui, P. Mirebeau, J.N. Demay, Industrial applications of polyaniline, Synth. Met. 101 (1999) 703–704.
[54] S. Bhadra, D. Khastgir, N.K. Singha, J.H. Lee, Progress in preparation, processing and applications of polyaniline, Prog. Polym. Sci. 34 (2009) 783–810.
[55] C.H. Teh, R. Rozaidi, D. Rusli, H.A. Sahrim, Synthesis and spectroscopic studies of DGEBA–grafted polyaniline, Polym.-Plast. Technol. Eng. 48 (2008) 17–24.
[56] A. Mirmohseni, G.G. Wallace, Preparation and characterization of processable electroactive polyanilin… polyvinyl alcohol composite, Polymer 44 (2003) 3523–3528.
[57] Q.M. Jia, J.B. Li, L. Wang, J.W. Zhu, M. Zheng, Electrically conductive epoxy resin composites containing polyaniline with different morphologies, Mater. Sci. Eng. A 448 (2007) 356–360.
[58] X. Cheng, V. Kumar, T. Yokozeki, T. Goto, T. Takahashi, J. Koyanagi, L. Wu, R. Wang, Highly conductive graphene oxide/polyaniline hybrid polymer nanocomposites with simultaneously improved mechanical properties, Compos. Appl. Sci. Manuf. 82 (2016) 100–107.
[59] S. Wang, Y. Zhou, Y. Liu, L. Wang, C. Gao, Enhanced thermoelectric properties of polyaniline/polypyrrole/carbon nanotube ternary composites by treatment with a secondary dopant using ferric chloride, J. Mater. Chem. C 8 (2020) 528–535.
[60] H. Yan, K. Kou, Enhanced thermoelectric properties in polyaniline composites with polyaniline-coated carbon nanotubes, J. Mater. Sci. 49 (2014) 1222–1228.
[61] M. Jaymand, Recent progress in chemical modification of polyaniline, Prog. Polym. Sci. 38 (2013) 1287–1306.
[62] S. Bhadra, S. Chattopadhyay, N.K. Singha, D. Khastgir, Improvement of conductivity of electrochemically synthesized polyaniline, J. Appl. Polym. Sci. 108 (2008) 57–64.
[63] Y. Haba, E. Segal, M. Narkis, G. Titelman, A. Siegmann, Polyaniline DBSA/polymer blends prepared via aqueous dispersions, Synth. Met. 110 (2000) 189–193.
[64] Y. Xia, J.M. Wiesinger, A.G. MacDiarmid, A.J. Epstein, Camphorsulfonic acid fully doped polyaniline emeraldine salt: conformations in different solvents studied by an ultraviolet/visible/near-infrared spectroscopic method, Chem. Mater. 7 (1995) 443–445.
[65] S.H. Park, K.-H. Shin, J.-Y. Kim, S.J. Yoo, K.J. Lee, J. Shin, J.W. Choi, J. Jang, Y.-E. Sung, The application of camphorsulfonic acid doped polyaniline films prepared on TCO-free glass for counter electrode of bifacial dye-sensitized solar cells, J. Photochem. Photobiol. Chem. 245 (2012) 1–8.
[66] C. Ma, L. Jiang, Y. Wang, F. Gang, N. Xu, T. Li, Z. Liu, Y. Chi, X. Wang, L. Zhao, Q. Feng, X. Sun, 3D printing of conductive tissue engineering scaffolds containing polypyrrole nanoparticles with different morphologies and concentrations, Materials 12 (2019) 2491.
[67] X. Ding, Y. Zhao, C. Hu, Y. Hu, Z. Dong, N. Chen, Z. Zhang, L. Qu, Spinning fabrication of graphene/polypyrrole composite fibers for all-solid-state, flexible fibriform supercapacitors, J. Mater. Chem. 2 (2014) 12355–12360.
[68] S. Dhibar, C.K. Das, Silver nanoparticles decorated polypyrrole/graphene nanocomposite: a potential candidate for next-generation supercapacitor electrode material, J. Appl. Polym. Sci. 134 (2017) 44724.
[69] H. Okuzaki, T. Kuwabara, K. Funasaka, T. Saido, Humidity-sensitive polypyrrole films for electro-active polymer actuators, Adv. Funct. Mater. 23 (2013) 4400–4407.
[70] P. Humpolíček, V. Kašpárková, J. Pacherník, J. Stejskal, P. Bober, Z. Capáková, K.A. Radaszkiewicz, I. Junkar, M. Lehocký, The biocompatibility of polyaniline and polypyrrole: a comparative study of their cytotoxicity, embryotoxicity and impurity profile, Mater. Sci. Eng. C 91 (2018) 303–310.
[71] H. Derakhshankhah, R. Mohammad-Rezaei, B. Massoumi, M. Abbasian, A. Rezaei, H. Samadian, M. Jaymand, Conducting polymer-based electrically conductive adhesive materials: design, fabrication, properties, and applications, Journal of Materials Science: Materials in Electronics 31 (2020) 10947–10961.
[72] H.K. Lim, S.O. Lee, K.J. Song, S.G. Kim, K.H. Kim, Synthesis and properties of soluble polypyrrole doped with dodecylbenzenesulfonate and combined with polymeric additive poly(ethylene glycol), J. Appl. Polym. Sci. 97 (2005) 1170–1175.
[73] Y. Shen, M. Wan, In situ doping polymerization of pyrrole with sulfonic acid as a dopant, Synth. Met. 96 (1998) 127–132.
[74] D.Y. Kim, J.Y. Lee, C.Y. Kim, E.T. Kang, K.L. Tan, Difference in doping behavior between polypyrrole films and powders, Synth. Met. 72 (1995) 243–248.
[75] Y.H. Lee, J.Y. Lee, D.S. Lee, A novel conducting soluble polypyrrole composite with a polymeric co-dopant, Synth. Met. 114 (2000) 347–353.
[76] T.y.V. Vernitskaya, O.N. Efimov, Polypyrrole: a conducting polymer; its synthesis, properties and applications, Russ. Chem. Rev. 66 (1997) 443–457.
[77] S. Sadki, P. Schottland, N. Brodie, G. Sabouraud, The mechanisms of pyrrole electropolymerization, Chem. Soc. Rev. 29 (2000) 283–293.
[78] J. Wang, Y. Xu, J. Zhu, P. Ren, Electrochemical in situ polymerization of reduced graphene oxide/polypyrrole composite with high power density, J. Power Sources 208 (2012) 138–143.
[79] C.M.G. Henríquez, G. del Carmen Pizarro Guerra, M.A.S. Vallejos, S.D.R. de la Fuente, M.T.U. Flores, L.M.R. Jimenez, In situ silver nanoparticle formation

embedded into a photopolymerized hydrogel with biocide properties, J. Nanostructure Chem. 4 (2014) 119–132.
[80] R. Nazar, S. Ronchetti, I. Roppolo, M. Sangermano, R.M. Bongiovanni, In situ synthesis of polymer embedded silver nanoparticles via photopolymerization, Macromol. Mater. Eng. 300 (2015) 226–233.
[81] E. Fantino, A. Chiappone, I. Roppolo, D. Manfredi, R. Bongiovanni, C.F. Pirri, F. Calignano, 3D printing of conductive complex structures with in situ generation of silver nanoparticles, Adv. Mat. 28 (2016) 3712–3717.
[82] N.S. Ilicheva, N.K. Kitaeva, V.R. Duflot, V.I. Kabanova, Synthesis and properties of electroconductive polymeric composite material based on polypyrrole, ISRN Polymer Science 2012 (2012) 320316.
[83] Z. Gao, L. Zhou, H. Huang, Exceptional anisotropy in conductivity and mechanical properties of poly-3-octylthiophene films, Thin Solid Films 347 (1999) 146–150.
[84] Y. Huang, H. Li, Z. Wang, M. Zhu, Z. Pei, Q. Xue, Y. Huang, C. Zhi, Nanostructured Polypyrrole as a flexible electrode material of supercapacitor, Nano Energy 22 (2016) 422–438.
[85] L. Liu, Y. Zhao, N. Jia, Q. Zhou, C. Zhao, M. Yan, Z. Jiang, Electrochemical fabrication and electronic behavior of polypyrrole nano-fiber array devices, Thin Solid Films 503 (2006) 241–245.
[86] C.K. Tan, D.J. Blackwood, Corrosion protection by multilayered conducting polymer coatings, Corrosion Sci. 45 (2003) 545–557.
[87] A.D. Bendrea, L. Cianga, I. Cianga, Review paper: progress in the field of conducting polymers for tissue engineering applications, J. Biomater. Appl. 26 (2011) 3–84.
[88] J. Wu, Q. Li, L. Fan, Z. Lan, P. Li, J. Lin, S. Hao, High-performance polypyrrole nanoparticles counter electrode for dye-sensitized solar cells, J. Power Sources 181 (2008) 172–176.
[89] C. Feng, L. Ma, F. Li, H. Mai, X. Lang, S. Fan, A polypyrrole/anthraquinone-2,6-disulphonic disodium salt (PPy/AQDS)-modified anode to improve performance of microbial fuel cells, Biosens. Bioelectron. 25 (2010) 1516–1520.
[90] Ö. Yavuz, M.K. Ram, M. Aldissi, P. Poddar, H. Srikanth, Polypyrrole composites for shielding applications, Synth. Met. 151 (2005) 211–217.
[91] T. Horii, H. Hikawa, M. Katsunuma, H. Okuzaki, Synthesis of highly conductive PEDOT:PSS and correlation with hierarchical structure, Polymer 140 (2018) 33–38.
[92] S.N. Karri, P. Srinivasan, Synthesis of PEDOT:PSS using benzoyl peroxide as an alternative oxidizing agent for ESD coating and electro-active material in supercapacitor, Mater. Sci. Energy Technol. 2 (2019) 208–215.
[93] P. Sakunpongpitiporn, K. Phasuksom, N. Paradee, A. Sirivat, Facile synthesis of highly conductive PEDOT:PSS via surfactant templates, RSC Adv. 9 (2019) 6363–6378.
[94] L. Ouyang, C. Musumeci, M.J. Jafari, T. Ederth, O. Inganäs, Imaging the phase separation between PEDOT and polyelectrolytes during processing of highly conductive PEDOT:PSS films, ACS Appl. Mater. Interfaces 7 (2015) 19764–19773.
[95] J.H. Lee, Y.R. Jeong, G. Lee, S.W. Jin, Y.H. Lee, S.Y. Hong, H. Park, J.W. Kim, S.-S. Lee, J.S. Ha, Highly conductive, stretchable, and transparent PEDOT:PSS electrodes fabricated with triblock copolymer additives and acid treatment, ACS Appl. Mater. Interfaces 10 (2018) 28027–28035.
[96] G.B. Tseghai, D.A. Mengistie, B. Malengier, K.A. Fante, L. Van Langenhove, PEDOT:PSS-Based conductive textiles and their applications, Sensors 20 (2020) 1881.
[97] S. Ghosh, N.A. Kouame, S. Remita, L. Ramos, F. Goubard, P.-H. Aubert, A. Dazzi, A. Deniset-Besseau, H. Remita, Visible-light active conducting polymer nanostructures with superior photocatalytic activity, Sci. Rep. 5 (2015) 18002.
[98] Y.H. Kim, C. Sachse, M.L. Machala, C. May, L. Müller-Meskamp, K. Leo, Highly conductive PEDOT:PSS electrode with optimized solvent and thermal post-treatment for ITO-free organic solar cells, Adv. Funct. Mater. 21 (2011) 1076–1081.
[99] A.M. Nardes, M. Kemerink, R.A.J. Janssen, Anisotropic hopping conduction in spin-coated PEDOT:PSS thin films, Phys. Rev. B 76 (2007) 085208.
[100] Y. Xia, J. Ouyang, PEDOT:PSS films with significantly enhanced conductivities induced by preferential solvation with cosolvents and their application in polymer photovoltaic cells, J. Mater. Chem. B 21 (2011) 4927–4936.
[101] H. Kim, Y.-J. Lee, G.-G. Park, S.-h. Park, Y. Choi, Y. Yoo, Fabrication of carbon paper containing PEDOT:PSS for use as a gas diffusion layer in proton exchange membrane fuel cells, Carbon 85 (2015) 422–428.
[102] F.B. Holness, A.D. Price, Direct ink writing of 3D conductive polyaniline structures and rheological modelling, Smart Mater. Struct. 27 (2017) 015006.
[103] K. Kurselis, R. Kiyan, V.N. Bagratashvili, V.K. Popov, B.N. Chichkov, 3D fabrication of all-polymer conductive microstructures by two photon polymerization, Opt. Express 21 (2013) 31029–31035.
[104] I. Salaoru, S. Maswoud, S. Paul, Inkjet printing of functional electronic memory cells: a step forward to green electronics, Micromachines 10 (2019) 417.
[105] H. Joo, S. Cho, Comparative studies on polyurethane composites filled with polyaniline and graphene for DLP-type 3D printing, Polymers 12 (2020) 67.
[106] K. Yamada, Y. Magori, S. Akimoto, J. Sone, Micro-nano 3D printing of electronically conductive polymers as a new process for achieving higher electronic conductivities, Microsyst. Technol. 25 (2019) 2051–2057.
[107] X. Wang, M. Jiang, Z. Zhou, J. Gou, D. Hui, 3D printing of polymer matrix composites: a review and prospective, Compos. B Eng. 110 (2017) 442–458.
[108] Z.-X. Low, Y.T. Chua, B.M. Ray, D. Mattia, I.S. Metcalfe, D.A. Patterson, Perspective on 3D printing of separation membranes and comparison to related unconventional fabrication techniques, J. Membr. Sci. 523 (2017) 596–613.
[109] E. Gutiérrez-Fernández, I.A. Gabaldón-Saucedo, M.C. García-Gutiérrez, A. Varea, A. Nogales, E. Rebollar, A. Vilà, T.A. Ezquerra, A. Cirera, Quantitative assessment by local probe methods of the mechanical and electrical properties of inkjet-printed PEDOT:PSS thin films over Indium Tin Oxide substrates, Org. Electron. 70 (2019) 258–263.
[110] F. Greco, A. Zucca, S. Taccola, A. Menciassi, T. Fujie, H. Haniuda, S. Takeoka, P. Dario, V. Mattoli, Ultra-thin conductive free-standing PEDOT/PSS nanofilms, Soft Matter 7 (2011) 10642–10650.
[111] G. Scordo, V. Bertana, L. Scaltrito, S. Ferrero, M. Cocuzza, S.L. Marasso, S. Romano, R. Sesana, F. Catania, C.F. Pirri, A novel highly electrically conductive composite resin for stereolithography, Mater. Today Commun. 19 (2019) 12–17.
[112] E. Saleh, B. Liu, J. Fernandez, C. Tuck, R. Wildman, I. Ashcroft, R. Hague, P. Dickens, The optimization of conductive inks for 3D inkjet printing, in: NIP & Digital Fabrication Conference, 2014.
[113] V. Kuzmenko, E. Karabulut, E. Pernevik, P. Enoksson, P. Gatenholm, Tailor-made conductive inks from cellulose nanofibrils for 3D printing of neural guidelines, Carbohydr. Polym. 189 (2018) 22–30.
[114] R.L. Truby, J.A. Lewis, Printing soft matter in three dimensions, Nature 540 (2016) 371–378.
[115] X. Mu, T. Bertron, C. Dunn, H. Qiao, J. Wu, Z. Zhao, C. Saldana, H.J. Qi, Porous polymeric materials by 3D printing of photocurable resin, Mater. Horizons 4 (2017) 442–449.
[116] K.A. Hamzah, C.K. Yeoh, M.M. Noor, P.L. Teh, Y.Y. Aw, S.A. Sazali, W.M.A. Wan Ibrahim, Mechanical properties and thermal and electrical conductivity of 3D printed ABS-copper ferrite composites via 3D printing technique, J. Thermoplast. Compos. Mater. 35 (2019) 3–16.
[117] C.R. Tubío, J. Azuaje, L. Escalante, A. Coelho, F. Guitián, E. Sotelo, A. Gil, 3D printing of a heterogeneous copper-based catalyst, J. Catal. 334 (2016) 110–115.
[118] H.-J. Choi, M.S. Kim, D. Ahn, S.Y. Yeo, S. Lee, Electrical percolation threshold of carbon black in a polymer matrix and its application to antistatic fibre, Sci. Rep. 9 (2019) 6338.
[119] A. Motaghi, A. Hrymak, G.H. Motlagh, Electrical conductivity and percolation threshold of hybrid carbon/polymer composites, J. Appl. Polym. Sci. 132 (2015), 41744.
[120] M. Rahaman, A. Aldalbahi, P. Govindasami, N.P. Khanam, S. Bhandari, P. Feng, T. Altalhi, A new insight in determining the percolation threshold of electrical conductivity for extrinsically conducting polymer composites through different sigmoidal models, Polymers 9 (2017) 527.
[121] A.J. Marsden, D.G. Papageorgiou, C. Vallés, A. Liscio, V. Palermo, M.A. Bissett, R.J. Young, I.A. Kinloch, Electrical percolation in graphene–polymer composites, 2D Mater. 5 (2018) 032003.
[122] P.H. Coelho, A.R. Morales, Electrical conductivity, percolation threshold and dispersion properties of PMMA nanocomposites of hybrid conducting fillers, in: 14th IEEE International Conference on Nanotechnology, 2014, pp. 706–710.
[123] V.B. Mohan, K. Jayaraman, D. Bhattacharyya, Hybridization of graphene-reinforced two polymer nanocomposites, Int. J. Smart Nano Mater. 7 (2016) 179.
[124] M.S. Mannoor, Z. Jiang, T. James, Y.L. Kong, K.A. Malatesta, W.O. Soboyejo, N. Verma, D.H. Gracias, M.C. McAlpine, 3D printed bionic ears, Nano Lett. 13 (2013) 2634–2639.
[125] Z. Lei, Z. Chen, H. Peng, Y. Shen, W. Feng, Y. Liu, Z. Zhang, Y. Chen, Fabrication of highly electrical conductive composite filaments for 3D-printing circuits, J. Mater. Sci. 53 (2018) 14495–14505.
[126] W.K.C. Yung, B. Sun, J. Huang, Y. Jin, Z. Meng, H.S. Choy, Z. Cai, G. Li, C.L. Ho, J. Yang, W.Y. Wong, Photochemical copper coating on 3D printed thermoplastics, Sci. Rep. 6 (2016) 31188.
[127] T. DebRoy, H.L. Wei, J.S. Zuback, T. Mukherjee, J.W. Elmer, J.O. Milewski, A.M. Beese, A. Wilson-Heid, A. De, W. Zhang, Additive manufacturing of metallic components – process, structure and properties, Prog. Mater. Sci. 92 (2018) 112–224.
[128] S. Jambhulkar, W. Xu, R. Franklin, D. Ravichandran, Y. Zhu, K. Song, Integrating 3D printing and self-assembly for layered polymer/nanoparticle microstructures as high-performance sensors, J. Mater. Chem. C 8 (2020) 9495–9501.
[129] J.C. Tan, H.Y. Low, Embedded electrical tracks in 3D printed objects by fused filament fabrication of highly conductive composites, Addit. Manuf. 23 (2018) 294–302.
[130] V. Vamvakaki, K. Tsagaraki, N. Chaniotakis, Carbon nanofiber-based glucose biosensor, Anal. Chem. 78 (2006) 5538–5542.
[131] I. Balberg, A comprehensive picture of the electrical phenomena in carbon blac⟨ polymer composites, Carbon 40 (2002) 139–143.
[132] F. Li, L. Qi, J. Yang, M. Xu, X. Luo, D. Ma, Polyurethane/conducting carbon black composites: structure, electric conductivity, strain recovery behavior, and their relationships, J. Appl. Polym. Sci. 75 (2000) 68–77.
[133] R. Sengupta, M. Bhattacharya, S. Bandyopadhyay, A.K. Bhowmick, A review on the mechanical and electrical properties of graphite and modified graphite reinforced polymer composites, Prog. Polym. Sci. 36 (2011) 638–670.
[134] M. Coroş, F. Pogăcean, L. Măgeruşan, C. Socaci, S. Pruneanu, A brief overview on synthesis and applications of graphene and graphene-based nanomaterials, Front. Mater. Sci. 13 (2019) 23–32.
[135] A.K. Geim, K.S. Novoselov, The rise of graphene, Nat. Mater. 6 (2007) 183–191.
[136] V.N. Popov, Carbon nanotubes: properties and application, Mater. Sci. Eng. R Rep. 43 (2004) 61–102.
[137] J. Czyżewski, P. Burzyński, K. Gaweł, J. Meisner, Rapid prototyping of electrically conductive components using 3D printing technology, J. Mater. Process. Technol. 209 (2009) 5281–5285.
[138] S. Khodabakhshi, P.F. Fulvio, E. Andreoli, Carbon black reborn: structure and chemistry for renewable energy harnessing, Carbon 162 (2020) 604–649.
[139] S.W. Kwok, K.H.H. Goh, Z.D. Tan, S.T.M. Tan, W.W. Tjiu, J.Y. Soh, Z.J.G. Ng, Y.Z. Chan, H.K. Hui, K.E.J. Goh, Electrically conductive filament for 3D-printed circuits and sensors, Appl. Mater. Today 9 (2017) 167–175.

[140] L.Y.W. Loh, U. Gupta, Y. Wang, C.C. Foo, J. Zhu, W.F. Lu, 3D printed metamaterial capacitive sensing array for universal jamming gripper and human joint wearables, Adv. Eng. Mater. 23 (2021) 2001082.
[141] A.H. Espera Jr., A.D. Valino, J.O. Palaganas, L. Souza, Q. Chen, R.C. Advincula, 3D printing of a robust polyamide-12-carbon black composite via selective laser sintering: thermal and electrical conductivity, Macromol. Mater. Eng. 304 (2019) 1800718.
[142] A.F. João, S.V.F. Castro, R.M. Cardoso, R.R. Gamela, D.P. Rocha, E.M. Richter, R.A.A. Muñoz, 3D printing pen using conductive filaments to fabricate affordable electrochemical sensors for trace metal monitoring, J. Electroanal. Chem. 876 (2020), 114701.
[143] W. Wu, H.-Y. Liu, Y. Kang, T. Zhang, S. Jiang, B. Li, J. Yin, J. Zhu, Synergistic combination of carbon-black and graphene for 3D printable stretchable conductors, Mater. Technol. (2020) 1–10.
[144] M. Dawoud, I. Taha, S.J. Ebeid, Strain sensing behaviour of 3D printed carbon black filled ABS, J. Manuf. Process. 35 (2018) 337–342.
[145] P.A. Eutionnat-Diffo, A. Cayla, Y. Chen, J. Guan, V. Nierstrasz, C. Campagne, Development of flexible and conductive immiscible thermoplastic/elastomer monofilament for smart textiles applications using 3D printing, Polymers 12 (2020) 2300.
[146] L. Lei, Z. Yao, J. Zhou, B. Wei, H. Fan, 3D printing of carbon black/polypropylene composites with excellent microwave absorption performance, Compos. Sci. Technol. 200 (2020) 108479.
[147] A. Mora, P. Verma, S. Kumar, Electrical conductivity of CNT/polymer composites: 3D printing, measurements and modeling, Compos. B Eng. 183 (2020), 107600.
[148] K. Gnanasekaran, T. Heijmans, S. van Bennekom, H. Woldhuis, S. Wijnia, G. de With, H. Friedrich, 3D printing of CNT- and graphene-based conductive polymer nanocomposites by fused deposition modeling, Appl. Mater. Today 9 (2017) 21–28.
[149] L.A. Chavez, J.E. Regis, L.C. Delfin, C.A. Garcia Rosales, H. Kim, N. Love, Y. Liu, Y. Lin, Electrical and mechanical tuning of 3D printed photopolymer–MWCNT nanocomposites through in situ dispersion, J. Appl. Polym. Sci. 136 (2019) 47600.
[150] V.B. Mohan, B.J. Krebs, D. Bhattacharyya, Development of novel highly conductive 3D printable hybrid polymer-graphene composites, Mater. Today Commun. 17 (2018) 554–561.
[151] X. Wei, D. Li, W. Jiang, Z. Gu, X. Wang, Z. Zhang, Z. Sun, 3D printable graphene composite, Sci. Rep. 5 (2015) 11181.
[152] B.G. Compton, N.S. Hmeidat, R.C. Pack, M.F. Heres, J.R. Sangoro, Electrical and mechanical properties of 3D-printed graphene-reinforced epoxy, JOM 70 (2018) 292–297.
[153] R.M. Hensleigh, H. Cui, J.S. Oakdale, J.C. Ye, P.G. Campbell, E.B. Duoss, C.M. Spadaccini, X. Zheng, M.A. Worsley, Additive manufacturing of complex micro-architected graphene aerogels, Mater. Horizons 5 (2018) 1035–1041.
[154] L. Feng, N. Xie, J. Zhong, Carbon nanofibers and their composites: a review of synthesizing, properties and applications, Materials 7 (2014) 3919–3945.
[155] S.S. Nakshatharan, J.G. Martinez, A. Punning, A. Aabloo, E.W.H. Jager, Soft parallel manipulator fabricated by additive manufacturing, Sensors and Actuators B: Chemical 305 (2020) 127355.
[156] Z. Hamouda, J. Wojkiewicz, A.A. Pud, L. Kone, B. Belaabed, S. Bergheul, T. Lasri, Dual-band elliptical planar conductive polymer antenna printed on a flexible substrate, IEEE Trans. Antenn. Propag. 63 (2015) 5864–5867.
[157] S.R. Dabbagh, M.R. Sarabi, R. Rahbarghazi, E. Sokullu, A.K. Yetisen, S. Tasoglu, 3D-printed microneedles in biomedical applications, iScience 24 (2020) 102012-102012.
[158] C. Micolini, F.B. Holness, J.A. Johnson, A.D. Price, Assessment of embedded conjugated polymer sensor arrays for potential load transmission measurement in orthopaedic implants, Sensors 17 (2017) 2768.
[159] D.N. Heo, S.-J. Lee, R. Timsina, X. Qiu, N.J. Castro, L.G. Zhang, Development of 3D printable conductive hydrogel with crystallized PEDOT:PSS for neural tissue engineering, Mater. Sci. Eng. C 99 (2019) 582–590.
[160] S. Vijayavenkataraman, S. Kannan, T. Cao, J.Y.H. Fuh, G. Sriram, W.F. Lu, 3D-Printed PCL/PPy conductive scaffolds as three-dimensional porous nerve guide conduits (NGCs) for peripheral nerve injury repair, Front. Bioeng. Biotechnol. 7 (2019) 266.
[161] B. Weng, X. Liu, R. Shepherd, G. Wallace, Inkjet printed polypyrrole/collagen scaffold: a combination of spatial control and electrical stimulation of PC12 cells, Synth. Met. 162 (2012) 1375–1380.
[162] A.E. Jakus, E.B. Secor, A.L. Rutz, S.W. Jordan, M.C. Hersam, R.N. Shah, Three-dimensional printing of high-content graphene scaffolds for electronic and biomedical applications, ACS Nano 9 (2015) 4636–4648.
[163] J. van den Brand, M. de Kok, M. Koetse, M. Cauwe, R. Verplancke, F. Bossuyt, M. Jablonski, J. Vanfleteren, Flexible and stretchable electronics for wearable health devices, Solid State Electron. 113 (2015) 116–120.
[164] W. Wu, Stretchable electronics: functional materials, fabrication strategies and applications, Adv. Mat.Sci. Technol. Adv. Mat. 20 (2019) 187–224.
[165] V. Yadav, G. Natu, R. Paily, Analysis of super-fine resolution printing of polyaniline and silver microstructures for electronic applications, in: IEEE Transactions on Components, Packaging and Manufacturing Technology, 2018, 1-1.
[166] A.T. ten Cate, C.H. Gaspar, H.L.K. Virtanen, R.S.A. Stevens, R.B.J. Koldeweij, J.T. Olkkonen, C.H.A. Rentrop, M.H. Smolander, Printed electronic switch on flexible substrates using printed microcapsules, J. Mater. Sci. 49 (2014) 5831–5837.
[167] J. Vaithilingam, E. Saleh, C. Tuck, R. Wildman, R. Hague, I. Ashcroft, P. Dickens, 3D-inkjet Printing of Flexible and Stretchable Electronics, 2015, pp. 1513–1526.
[168] A.I. Hofmann, I. Östergren, Y. Kim, S. Fauth, M. Craighero, M.-H. Yoon, A. Lund, C. Müller, All-polymer conducting fibers and 3D prints via melt processing and templated polymerization, ACS Appl. Mater. Interfaces 12 (2020) 8713–8721.
[169] L. Li, Z. Lou, W. Han, D. Chen, K. Jiang, G. Shen, Highly stretchable micro-supercapacitor arrays with hybrid MWCNT/PANI electrodes, Adv. Mater. Technol. 2 (2017) 1600282.
[170] S. Duan, K. Yang, Z. Wang, M. Chen, L. Zhang, H. Zhang, C. Li, Fabrication of highly stretchable conductors based on 3D printed porous poly(dimethylsiloxane) and conductive carbon nanotubes/graphene network, ACS Appl. Mater. Interfaces 8 (2016) 2187–2192.
[171] D. Zhang, B. Chi, B. Li, Z. Gao, Y. Du, J. Guo, J. Wei, Fabrication of highly conductive graphene flexible circuits by 3D printing, Synth. Met. 217 (2016) 79–86.
[172] J. Janata, M. Josowicz, Conducting polymers in electronic chemical sensors, Nat. Mater. 2 (2003) 19–24.
[173] Y. Wang, A. Liu, Y. Han, T. Li, Sensors based on conductive polymers and their composites: a review, Polym. Int. 69 (2020) 7–17.
[174] H. Devaraj, K.C. Aw, J. Travas-Sejdic, R.N. Sharma, Low velocity digital air flow sensor from 3D printed PEDOT:PSS micro-hair structures, 2015 Transducers - 2015, in: 18th International Conference on Solid-State Sensors, Actuators and Microsystems (TRANSDUCERS), 2015, pp. 1097–1100.
[175] G. Tarabella, S.L. Marasso, V. Bertana, D. Vurro, P. D'Angelo, S. Iannotta, M. Cocuzza, Multifunctional operation of an organic device with three-dimensional architecture, Materials 12 (2019) 1357.
[176] Z. Wang, W. Gao, Q. Zhang, K. Zheng, J. Xu, W. Xu, E. Shang, J. Jiang, J. Zhang, Y. Liu, 3D-Printed graphene/polydimethylsiloxane composites for stretchable and strain-insensitive temperature sensors, ACS Appl. Mater. Interfaces 11 (2019) 1344–1352.
[177] K. Chizari, M.A. Daoud, A.R. Ravindran, D. Therriault, 3D printing of highly conductive nanocomposites for the functional optimization of liquid sensors, Small 12 (2016) 6076–6082.
[178] Y. Zhao, B. Liu, L. Pan, G. Yu, 3D nanostructured conductive polymer hydrogels for high-performance electrochemical devices, Energy Environ. Sci. 6 (2013) 2856–2870.
[179] A. Rudge, J. Davey, I. Raistrick, S. Gottesfeld, J.P. Ferraris, Conducting polymers as active materials in electrochemical capacitors, J. Power Sources 47 (1994) 89–107.
[180] R. Xing, Y. Xia, R. Huang, W. Qi, R. Su, Z. He, Three-dimensional printing of black phosphorous/polypyrrole electrode for energy storage using thermoresponsive ink, Chem. Commun. 56 (2020) 3115–3118.
[181] P. Dou, Z. Liu, Z. Cao, J. Zheng, C. Wang, X. Xu, Rapid synthesis of hierarchical nanostructured Polyaniline hydrogel for high power density energy storage application and three-dimensional multilayers printing, J. Mater. Sci. 51 (2016) 4274–4282.
[182] Z. Qi, J. Ye, W. Chen, J. Biener, E.B. Duoss, C.M. Spadaccini, M.A. Worsley, C. Zhu, 3D-Printed, superelastic polypyrrole–graphene electrodes with ultrahigh areal capacitance for electrochemical energy storage, Adv. Mater. Technol. 3 (2018) 1800053.
[183] G.H. Shim, M. Han, J. Sharp-Norton, S. Creager, S. Foulger, Inkjet-printed electrochromic devices utilizing polyaniline–silica and poly(3,4-ethylenedioxythiophene)–silica colloidal composite particles, J. Mater. Chem. 18 (2008) 594–601.
[184] X. Lu, T. Zhao, X. Ji, J. Hu, T. Li, X. Lin, W. Huang, 3D printing well organized porous iron-nickel/polyaniline nanocages multiscale supercapacitor, J. Alloys Compd. 760 (2018) 78–83.
[185] G. Kaur, R. Adhikari, P. Cass, M. Bown, P. Gunatillake, Electrically conductive polymers and composites for biomedical applications, RSC Adv. 5 (2015) 37553–37567.
[186] K.K. Kanazawa, A.F. Diaz, M.T. Krounbi, G.B. Street, Electrical properties of pyrrole and its copolymers, Synth. Met. 4 (1981) 119–130.
[187] K.M. Ziadan, W.T. Saadon, Study of the electrical characteristics of polyaniline prepeared by electrochemical polymerization, Energy Procedia 19 (2012) 71–79.
[188] W. ŁUzny, E. Bańka, Relations between the structure and electric conductivity of polyaniline protonated with camphorsulfonic acid, Macromolecules 33 (2000) 425–429.
[189] L. Groenendaal, F. Jonas, D. Freitag, H. Pielartzik, J.R. Reynolds, Poly(3,4-ethylenedioxythiophene) and its derivatives: Past, present, and future, Adv. Mater. 12 (2000) 481–494.
[190] Z. Yu, Y. Xia, D. Du, J. Ouyang, PEDOT:PSS films with metallic conductivity through a treatment with common organic solutions of organic salts and their application as a transparent electrode of polymer solar cells, ACS Appl. Mater. Interfaces 8 (2016) 11629–11638.
[191] X. Ding, R. Jia, Z. Gan, Y. Du, D. Wang, X. Xu, Tough and conductive polymer hydrogel based on double network for photo-curing 3D printing, Mater. Res. Express 7 (2020) 055304.
[192] H. Han, S. Cho, Fabrication of conducting polyacrylate resin solution with polyaniline nanofiber and graphene for conductive 3D printing application, Polymers 10 (2018) 1003.
[193] R. Hong, Z. Zhao, J. Leng, J. Wu, J. Zhang, Two-step approach based on selective laser sintering for high performance carbon black/ polyamide 12

composite with 3D segregated conductive network, Compos. Part B Eng. 176 (2019) 107214.
[194] S.R. Athreya, K. Kalaitzidou, S. Das, Processing and characterization of a carbon black-filled electrically conductive Nylon-12 nanocomposite produced by selective laser sintering, Mater. Sci. Eng. A 527 (2010) 2637–2642.
[195] G. Gonzalez, A. Chiappone, I. Roppolo, E. Fantino, V. Bertana, F. Perrucci, L. Scaltrito, F. Pirri, M. Sangermano, Development of 3D printable formulations containing CNT with enhanced electrical properties, Polymer 109 (2017) 246–253.
[196] L.L. Lebel, B. Aissa, M.A. El Khakani, D. Therriault, Ultravolet-assisted direct-write fabrication of carbon nanotube/polymer nanocomposite microcoils, Adv. Mater. 22 (2010) 592–596.
[197] C.B. Sweeney, B.A. Lackey, M.J. Pospisil, T.C. Achee, V.K. Hicks, A.G. Moran, B.R. Teipel, M.A. Saed, M.J. Green, Welding of 3D-printed carbon nanotube–polymer composites by locally induced microwave heating, Sci. Adv. 3 (2017) 700262.
[198] R. Paz, R. Moriche, M. Monzón, J. García, Influence of manufacturing parameters and post processing on the electrical conductivity of extrusion-based 3D printed nanocomposite parts, Polymers 12 (2020) 733.
[199] A. Chiappone, I. Roppolo, E. Naretto, E. Fantino, F. Calignano, M. Sangermano, F. Pirri, Study of graphene oxide-based 3D printable composites: Effect of the in situ reduction, Compos. Part B Eng. 124 (2017) 9–15.
[200] G. McKerricher, D. Titterington, A. Shamim, A fully inkjet-printed 3-D honeycomb-inspired patch antenna, IEEE Antennas Wirel. Propag. Lett. 15 (2016) 544–547.
[201] J.F. Christ, N. Aliheidari, A. Ameli, P. Pötschke, 3D printed highly elastic strain sensors of multiwalled carbon nanotube/thermoplastic polyurethane nanocomposites, Mater. Design 131 (2017) 394–401.
[202] Q. Mu, L. Wang, C.K. Dunn, X. Kuang, F. Duan, Z. Zhang, H.J. Qi, T. Wang, Digital light processing 3D printing of conductive complex structures, Addit. Manuf. 18 (2017) 74–83.